

# A remotely sensed study of the impact of meteorological parameters on vegetation for the eastern basins of Afghanistan

**Ahmad Farid Nabizada**

Yazd University

**Iman Rousta** (✉ [irousta@yazd.ac.ir](mailto:irousta@yazd.ac.ir))

Yazd University

**Gholamali Mozaffari**

Yazd University

**Marjan Dalvi**

University of Iceland

**Haraldur Olafsson**

University of Iceland

**Anna Siedliska**

Polish Academy of Sciences

**Piotr Baranowski**

Polish Academy of Sciences

**Przemysław Tkaczyk**

University of Life Sciences in Lublin

**Jaromir Krzyszczyk**

Polish Academy of Sciences

---

## Research Article

**Keywords:** remote sensing, vegetation coverage, drought, meteorological conditions, Afghanistan

**Posted Date:** November 18th, 2022

**DOI:** <https://doi.org/10.21203/rs.3.rs-2267890/v1>

**License:**  This work is licensed under a Creative Commons Attribution 4.0 International License.

[Read Full License](#)

**Additional Declarations:** No competing interests reported.

---

**Version of Record:** A version of this preprint was published at Earth Science Informatics on February 23rd, 2023. See the published version at <https://doi.org/10.1007/s12145-023-00965-1>.

# Abstract

Despite the importance of the Amu Darya and Kabul River Basins as a region in which more than 15 million people live, and its vulnerability to global warming, only several studies addressed the issue of the linkage of meteorological parameters on vegetation for the eastern basins of Afghanistan. In this study, data from the MODIS, Global Precipitation Measurement Mission (GPM), and Global Land Data Assimilation System (GLDAS) was used for the period from 2000 to 2021. The study utilized several indices, such as Precipitation Condition Index (PCI), Temperature Condition Index (TCI), Soil Moisture Condition Index (SMCI), and Microwave Integrated Drought Index (MIDI). The relationships between meteorological quantities, drought conditions, and vegetation variations were examined by analyzing the anomalies and using regression methods. The results showed that the years 2000, 2001, and 2008 had the lowest vegetation coverage (VC) (56, 56, and 55% of the study area, respectively). On the other hand, the years 2010, 2013, 2016, and 2020 had the highest VC (71, 71, 72, and 72% of the study area, respectively). The trend of the VC for the eastern basins of Afghanistan for the period from 2000 to 2021 was upward. High correlations between VC and soil moisture ( $R = 0.70$ ,  $p = 0.0004$ ), and precipitation ( $R = 0.5$ ,  $p = 0.008$ ) were found, whereas no significant correlation was found between VC and drought index MIDI. It was revealed that soil moisture, precipitation, land surface temperature, and area under meteorological drought conditions explained 45% of annual VC variability.

## 1. Introduction

Abnormal climatic conditions related to climate change have been associated with the effects of human activities over the past few decades. They lead to numerous environmental and ecological problems, such as air pollution, dust storm, biodiversity loss, soil erosion, and vegetation degradation (Li et al. 2022a; Zhao et al. 2022b; Zhou et al. 2021). Therefore, the knowledge of how climate change affects different ecosystems has an important role in the protection and management of vegetation cover (Tian et al. 2021b).

Vegetation occupies almost half of the planet and plays an important role in providing food, fiber, and fuel, supporting animal biodiversity, maintaining climate quality, and supporting ecological processes that preserve ecosystems and landscapes (Hu et al. 2022; Li et al. 2021; Li et al. 2022b; Yang et al. 2022). Vegetation is one of the important components of the terrestrial ecosystem, which plays an effective role in preventing desertification and also plays a key role in providing various ecosystem services to adapt and mitigate climate change; Additionally, every change in vegetation affects the climate of the region, especially temperature and air quality, through its influence on net radiation, energy partitioning, conversion of precipitation to runoff (Chen et al. 2022; Liu et al. 2020; Mansourmoghaddam et al. 2022b; Zhu et al. 2022), soil moisture (Zhang et al. 2019b), evaporation, and transpiration (Najmuddin et al. 2017). Since global climate change has become a major topic of discussion today, the relationship between vegetation and meteorological factors is of great importance in ecological studies (Gao et al. 2012).

Remote sensing can continuously and systematically deliver information on the water cycle and vegetation variations and therefore, remote sensing drought indicators can be used for spatial and temporal drought monitoring (Mansourmoghaddam et al. 2022a; Wang et al. 2021; Xie et al. 2021a; Xie et al. 2021b; Yin et al. 2022b). Remote sensing is of particular importance in applications requiring actual and constantly updated information. Due to various spectral ranges and data availability, the use of remote sensing data is one of the best ways to prepare vegetation (Tian et al. 2021a; Yin et al. 2022a) and soil moisture (Zhao et al. 2021; Zhao et al. 2020) maps.

The NDVI index has become one of the most popular and commonly used indicators to monitor vegetation due to its universality and simple mathematical formula (Rousta et al. 2020a). According to Huang et al. (Huang et al. 2021b), the number of articles using the NDVI index to monitor changes in vegetation increased from 795 in 1990, through 3361 in 2000, to 12,618 in 2010 (Huang et al. 2021a). The NDVI index is widely used in studies related to vegetation classification, and soil erosion risk assessment, because soil erosion decreases with increasing vegetation cover (Zhongming et al. 2010). By correlating NDVI data with the meteorological parameters using the long-term time series for the specific study area it can be checked how climate change affects the growth of vegetation (Li and Kafatos 2000). Also, such studies can be performed to check whether persistent drought conditions occur in a given area and how they affect vegetation.

The period of instability from dry weather conditions, which leads to water scarcity, is simply known as drought (Xu et al. 2022b). Drought is a very complex and not well-understood phenomenon. It causes social and environmental problems, and it leads to immeasurable economic losses (Zhao et al. 2022a). Drought is a serious natural hazard, especially in regions with arid and semi-arid climates (Ali et al. 2019). Compared to other natural phenomena, drought affects wider areas over a longer period, thus causing much more damage than other natural disasters such as floods and earthquakes (Zhang et al. 2022). The study of climate change and the identification of years of drought are valuable for the management of water resources and vegetation, especially in areas with dry spell occurrence (Jawadi et al.)

Afghanistan is a mountainous country with spatially and temporally varying ecological conditions. Mountainous areas are prone to the effects of climate change, which intensifies the pressure on natural and human systems (Omerkhil et al. 2020). Climate changes have caused short-term and long-term droughts that have severely affected Afghanistan's economy. According to the International Disaster Management Agency (IDD), droughts accounted for only 5 percent of natural disasters but affected about 30 percent of the population (Ji and Peters 2005). There are two main types of drought in Afghanistan: meteorological drought (usually accompanied by a lack of rainfall) and hydrological drought (usually associated with a lack of surface and groundwater flow, potentially originating in the wider river basin region) (Gao et al. 2021; Liu et al. 2022; Munyasya et al. 2022; Quan et al. 2021; Zhang et al. 2019c). These issues may also be combined with land and crop management practices, leading to agricultural drought. Currently, Afghanistan is facing significant drought issues that have a direct impact on the livelihoods and the economy of the country.

The vegetation in Afghanistan has been severely affected by human activities, climate change, and drought, which resulted in the naturally occurring vegetation preserved intact only in a few high mountain areas and abnormally dry deserts (Rousta et al. 2020a). Such a situation additionally contributes to Afghanistan's vulnerability to the effects of climate change (Akhundzadah et al. 2020). In Afghanistan, the combined effects of climate change and four decades of civil war have destroyed vegetation and infrastructure, leading to the underdevelopment of the country. The high dependence of the majority of the country's people on small and large-scale agriculture means that due to the country's dry climate and the low adaptation capacity of farmers climate change creates major problems to deal with (Xu et al. 2022a). The arid and semi-arid climate of the eastern basins of Afghanistan implies that this area can be strongly affected by short and long-term fluctuations of meteorological parameters, which as a result will endanger human living conditions (Aich et al. 2017). In Afghanistan, where a large part of the population is engaged in the agriculture sector, assessing the impacts of climate change and drought on vegetation is crucial for the implementation of sustainable agricultural practices. This is especially important for different crops that are grown annually and seasonally, for example, wheat produced in the north, northeast, and eastern regions of the country (Shroder 2014).

In Afghanistan, due to security problems and the lack of stations monitoring weather, not many studies have been performed on the correlation between meteorological parameters and vegetation, and only a few research were done using remote sensing data (Rousta et al. 2020a). Therefore, the investigation of the impact of weather and climate change on vegetation for proper management and ensuring the stability of vegetation, being of particular importance for the eastern basins of Afghanistan, is still required and expected.

The presented study has been conducted to monitor the fluctuations of vegetation conditions and to assess their relationship with meteorological parameters and drought conditions in the period of 2000–2021 in the eastern basins of Afghanistan. The main objectives of this study were a) to determine the trend of vegetation changes between the years (2000–2021) in the eastern basin of Afghanistan, b) to analyze the past trends in drought from the perspective of meteorology, and c) to determine the relationship between vegetation, drought and meteorological parameters for the eastern basins of Afghanistan. The results of this study can be used by governmental agencies, such as the Ministry of Agriculture, to identify dry and wet years, as well as to determine the trend of changes in meteorological parameters and vegetation for the period 2000–2021.

## **2. Materials And Methods**

### **2.1. Study area**

The study has been performed for the eastern basins of Afghanistan (Fig. 1), namely the Amu Darya Basin (ADB) and the Kabul River Basin (KRB), with a total area of 163,840 km<sup>2</sup>. The Amu Darya Basin, with an area of 90,692 km<sup>2</sup>, is bordered by Tajikistan from the north, and Pakistan from the southeast. The total annual water flowing through this basin is 82 billion m<sup>3</sup>, of which 61% comes from Tajikistan,

30% from Afghanistan, and the remaining 9% from Uzbekistan and Turkmenistan. Important Amu Darya tributaries include the Wakhan, Kokcha, Kunduz, Andarab, Khenjan, and Punjab rivers in Afghanistan. The population living in this basin was reported to be about 4.5 million people in 2015. According to the division of the Ministry of Energy and Water, it is divided into 7 sub-basins: Upper Five, Lower Five, Kokcheh, Taloqan, Upper Kunduz, Lower Kunduz, and Lower Amu (Maharjan et al. 2021).

The Kabul River Basin, with an area of 72,843 km<sup>2</sup> is located in the eastern part of Afghanistan and is part of the Indus River Basin, which is common between Afghanistan and Pakistan. A part of this basin includes the Kabul and Kunar river basins, with an area of 53,832 km<sup>2</sup>. Kabul River Basin is the second largest basin in Afghanistan after the Amu Darya and is divided into 13 sub-basins: Upper Panjshir, Lower Panjshir, Ghorband, Central Kabul, Maidan, Logar, Laghman, Lower Kabul, Kunar, Parun, North, Khorram, and Gomel. The population living in this catchment area is estimated to be about 12.1 million in 2015 (Maharjan et al. 2021).

Most of the Amu Darya basin is mountainous with snow/glacier fed rivers flowing in steep terrain. The rangeland on the mountain side is grazed by farm animals and nomads during the warm summer months (Cesaro et al. 2019). The northern part of KRB contains mountains with high elevations (Najmuddin et al. 2018). The lowlands of KRB are the most suitable land for agriculture. The farms are mainly located in the central and eastern parts of the KRB, Agriculture and livestock are the main source of livelihoods in the KRB. Agriculture is largely irrigated and shares around one-fifth of the total irrigated land in the country. The river basin also holds around two-thirds of the total forest resources in the count (Najmuddin et al. 2017).

Table 1  
Land Cover type of Kabul River Basin and Amu Darya Basin of Afghanistan.

Land Cover type	Area (km <sup>2</sup> )
Urban and Built-Up Land	168.9
Dryland Cropland and Pasture	9497.6
Irrigated Cropland and Pasture	12009.2
Cropland/Grassland Mosaic	1619.5
Cropland/Woodland Mosaic	7828.2
Grassland	44105.9
Shrubland	58974.3
Mixed Shrubland/Grassland	3794.8
Savanna	450.3
Deciduous Broadleaf Forest	71.3
Deciduous Needleleaf Forest	1.4
Evergreen Broadleaf Forest	0.7
Evergreen Needleleaf Forest	52.0
Mixed Forest	71.3
Water Bodies	485.2
Wooded Wetland	64.1
Barren or Sparsely Vegetated	11655.8
Wooded Tundra	12091.8
Snow or Ice	3749.2

Climate change has already affected agriculture and vegetation in the ADB and KRB. Due to earlier snow melting spring floods increase in size and the risk of the shortage of water occurs more often in summer and early autumn in years of drought (Klemm and Shobair 2010). In 2013, annual precipitation in the KRB was 327 mm at downstream, with a usual fringe effect of the Indian monsoon coming from the South Asian Himalayas, and around 418 mm at upstream. The mean annual temperature at the central upstream and downstream locations were 13°C and 23 °C, respectively (Akhtar et al. 2018). Table 1 and Fig. 2 presents the land cover types of ADB and KRB watersheds, together with their area (km<sup>2</sup>) retrieved from Moderate resolution imaging spectroradiometer (MODIS)\_ MCD12Q1 images according to the International Geosphere-Biosphere Programme (IGBP) classification (Loveland et al. 1999). The figure

shows that most of the study area is covered by croplands and grasslands (18 and 26% of study area, respectively).

## 2.2. Data

In the present study, the vegetation coverage variability for the eastern basins of Afghanistan was investigated for the period 2000–2021, and the impact of such factors as land surface temperature (LST), precipitation, soil moisture, and drought on vegetation coverage was assessed using regression methods. The summary of the sources of the remote sensing data used in this study is provided in Table 2, while the flowchart of data processing is presented in Fig. 3. All satellite-born statistics of the surfaces belong to the bright days (hours) only.

Table 2  
Remote sensing data used in this study.

Data	Source	Spatial resolution	Temporal resolution	File Format
Normalized Difference Vegetation Index (MOD13Q1)	MODIS packages in GEE	250 m	16 days	Geo tif
MODIS Land Surface Temperature (MOD11A2)	MODIS packages in GEE	1 km	8 days	Geo tif
Global Precipitation Measurement (GPM)	GPM packages in GEE	0.1° arc degree	30 minutes	Geo tif
Global Land Data Assimilation System (GLDAS) soil moisture (in soil layer of 0–10 cm )	GLDAS packages in GEE	1°	3 hours	NC file

### 2.2.1. Normalized Difference Vegetation Index (NDVI) data

The Normalized Difference Vegetation Index (NDVI) is one of the most important and widely used vegetation indicators and its application in satellite assessment for global vegetation monitoring has been well proven in the two last decades (Leprieur et al. 2000). It is commonly used as a detector of surrounding greenness areas and in epidemiological studies to investigate the health effects of green space in urban environments (Gascon et al. 2016). The NDVI is the index that is less affected by factors such as topography and brightness than other vegetation indices and it indicates the level of photosynthetic activity of the vegetation (Mansourmoghaddam et al. 2022e):



$$NDVI = \frac{R_{nir} - R_{red}}{R_{nir} + R_{red}}$$

1  
,

where  $R_{red}$  and  $R_{nir}$  represent surface reflectance averaged over visible (RED) ( $\lambda \sim 0.65 \mu\text{m}$ ) and near-infrared (NIR) ( $\lambda \sim 0.85 \mu\text{m}$ ) regions of the spectrum (Mansourmoghaddam et al. 2022d). The range of NDVI values is between  $-1$  and  $1$ , with the vegetation having NDVI between  $0.2$ - $1.0$ , while the values lesser than  $0.2$  indicate areas without vegetation cover, usually barren, or with rock, snow, water, or ice (Mahmood et al. 2022; Rousta et al. 2022b; Rousta et al. 2020a; Rousta et al. 2020b).

In this study, the time-series of the NDVI 16-Day L3 Global 250 m from MOD13Q1 MODIS product (Testa et al. 2014) for a period from January 2000 to December 2021 (22 years, 528 images in total) have been downloaded using the Google Earth Engine (GEE) platform. The data was converted to the spatial resolution of 1 km using the bicubic method.

To obtain the yearly values of the NDVI the data were averaged as:

$$\text{YearlyNDVI} = \frac{\sum_{i=1}^{23} \text{NDVI}_i}{23}$$

2  
,

where  $i$  is consecutively numbering the timely ordered images from a specific year. Based on the NDVI, vegetation coverage was calculated as the area with any type of vegetation by summation of the number of the pixels with  $\text{NDVI} > 0.2$  and multiplying their number by the area of one pixel.

The uncertainty estimation of the area of vegetation cover in this research was related to the conditions in the study area. As the study area is mountainous with unpredictable weather, the major contribution to NDVI uncertainty comes from topographic and atmospheric factors (Borgogno-Mondino et al. 2016). Additionally, the thresholding of  $\text{NDVI} > 0.2$  and considering that values above are representative for vegetation, and the assumption that all the area of a pixel with  $\text{NDVI} > 0.2$  is treated as the area covered with vegetation is a very crude approach.

## 2.2.2. Land Surface Temperature (LST) data

In the study, the time-series of the LSTDay-8Day-1km from MOD11A2 MODIS product with a spatial resolution of 1 km and temporal resolution of 8 days data was used. The data from 2000 to 2021 (22 years, 1056 images in total) were downloaded using the Google Earth Engine (GEE) platform and then averaged to yearly values using:

$$\text{Yearly LST} = \frac{\sum_{i=1}^{46} \text{LST}_i}{46}, (3)$$

## 2.2.3. Precipitation data

The precipitation was derived from the Global Precipitation Measurement (GPM) product. It is an international satellite mission to provide next-generation observations of precipitation and snow worldwide every three hours (Huffman et al. 2015). The GPM data were obtained using the Google Earth Engine (GEE) platform and then averaged to yearly values.

## 2.2.4. Soil moisture data

The purpose of the Global Land Data Assimilation System (GLDAS) was to employ a source of data for the assessment of the environmental and food security in developing countries, such as Afghanistan, that do not have access to terrestrial data (McNally et al. 2017). The overall goal of the GLDAS model was to drive multiple offline LSMs and integrate large amounts of observation-based data, to be implemented globally with high resolution. GLDAS offers a product with a spatial resolution of 0.25° and 1° and a temporal resolution of 3 hourly. The data is available from January 1948 up to the present (Bi et al. 2016). In this study, the Global Land Data Assimilation System (GLDAS) data was used to obtain information on the soil moisture from a depth of 0–10 cm. To match the same spatial resolution as for the other data, the bicubic method has been used to re-sample the soil moisture data to a 1km grid. Such resampling was needed to integrate soil moisture data with other data into the Microwave Integrated Drought Index (MIDI) (they had to have the same spatial resolution). The GLDAS dataset was accessed using the GEE.

## 2.3. Methods

### 2.3.1. Vegetation Condition Index (VCI)

Since 2014, Kenya's National Drought Management Authority (NDMA) uses the vegetation condition index (VCI) as the basis for providing disaster contingency funds to counties in drought conditions (Mansourmoghaddam et al. 2022c). VCI is a normalized pixel-based NDVI to separate long-term ecosystem changes from short-term climate-related NDVI fluctuations and to reflect relative changes in vegetation conditions from very poor to optimal (Liu and Kogan 1996). VCI compares the current time vegetation with the minimum long-term NDVI and shows how close the current time step is to the long-term minimum NDVI, taking into account the difference between the maximum (indicating the best conditions of vegetative growth) and minimum values (indicating the worst conditions of vegetative growth), which reflect somehow the conditions of the local vegetation (Karnieli et al. 2006). The range of VCI is between 0 and 1, with smaller VCI values indicating worse vegetation growth conditions and, at the same time, higher degrees of drought. Based on the literature regarding aridity classification standards, VCI lower than 0.5 indicates drought conditions (Sha et al. 2013). VCI is defined as:

$$VCI = \frac{NDVI_i - NDVI_{\min}}{NDVI_{\max} - NDVI_{\min}}$$

4

where 'min' and 'max' are multiyear maximum and minimum, respectively, and 'i' denotes the current time step.

### 2.3.2. Temperature Condition Index (TCI)

The Temperature Condition Index (TCI) is one of the indicators of drought, which assumes that the occurrence of drought phenomenon reduces soil moisture and creates thermal stress on the surface of the earth, which results in the monthly LST in the year of drought greater than for the same month in normal years (Du et al. 2013). It is calculated as:

$$TCI = \frac{LST_i - LST_{\min}}{LST_{\max} - LST_{\min}}$$

5

where 'min' and 'max' are multiyear maximum and minimum, respectively, and 'i' denotes the current time step.

### 2.3.3. Precipitation Condition Index (PCI)

Precipitation Condition Index (PCI) was used to evaluate the variation of precipitation and drought conditions from GPM DATA (Wang et al. 2019). Many previous studies used PCI for monitoring drought instead of Standard Precipitation Index (SPI) and Standardised Precipitation Evapotranspiration Index (SPEI) (Baig et al. 2020; Han et al. 2020; Wang et al. 2019), and indicate that it is very reliable index. It is defined as:

$$PCI = \frac{P_i - P_{\min}}{P_{\max} - P_{\min}}$$

6

where 'min' and 'max' are multiyear maximum and minimum, respectively, and 'i' denotes the current time step.

### 2.3.4. Soil Moisture Condition Index (SMCI)

Soil moisture data (GLDAS) was used to drive the soil moisture condition index (SMCI) as:

$$SMCI = \frac{SM_i - SM_{\min}}{SM_{\max} - SM_{\min}}$$

7

where 'min' and 'max' are multiyear maximum and minimum, respectively, and 'i' denotes the current time step.

### 2.3.5. Microwave Integrated Drought Index (MIDI)

The MIDI is a reliable index for monitoring drought, which integrates the precipitation condition index (PCI), soil moisture condition index (SMCI), and temperature condition index (TCI) (Zhang et al. 2019a). These indices are linearly scaled between 0 and 1 using the absolute maximum and minimum values for the same month based on microwave-derived precipitation, soil moisture, and land surface temperature (LST), respectively. Microwave Integrated Drought Index (MIDI) integrates the PCI, TCI, and SMCI indices with flexible weights  $\alpha$ ,  $\beta$ , and  $\gamma$  (Wei et al. 2021):

$$MIDI = \alpha PCI + \beta SMCI + \gamma TCI$$

8

where  $\alpha + \beta + \gamma = 1$ . In this study, based on the literature recommendations, in which the best correlation with the short-term Standard Precipitation Index (SPI) was obtained (Zhang et al. 2019a), weights  $\alpha = 0.5$ ,  $\beta = 0.3$ , and  $\gamma = 0.2$  were used. The range of MIDI values is between 0 and 1, where the value between 0 to 0.1 indicates extreme drought conditions, the value in the range from 0.11 to 0.2 indicates severe drought conditions, from 0.21 to 0.3 - moderate drought conditions, from 0.31 to 0.4 - low drought conditions and from 0.41 to 1.0 indicates that area under consideration is not experiencing drought.

### 2.3.6. Z-score calculation

Z-score, also known as the standardized anomaly, informs how large the deviations of the quantity under consideration are. The Z-score is calculated using the formula (Zhao et al. 2019):

$$Z_{ij} = \frac{X_{ij} - U}{\sigma_{ij}}$$

9

where  $i$  represents the assessed period and  $j$  stands for the time scale,  $X_{ij}$  is an analyzed parameter in a given year,  $U$  represents the mean value for the analyzed statistical period, whereas  $\sigma_{ij}$  indicates the standard deviation. Positive values of the standardized anomaly indicate that the values under consideration are larger than the mean, the negative values of the standardized anomaly indicate that the

values are smaller than the mean, and the values  $>|2|$  indicate that the result is abnormal (Wu and Onipchenko 2007).

## 2.3.6. Correlations calculation

The correlation coefficients were calculated using Pearson correlation. It measures the strength of the linear relationship between two (dependent and independent) variables (Zhou et al. 2016). It has a value between  $-1$  to  $1$ , with  $-1$  meaning a total negative linear correlation,  $0$  meaning that two quantities are not correlated, and  $+1$  meaning a total positive correlation. The Pearson correlation is the first formal measure of correlation and it is still one of the most widely used measure of relationships between variables (Lee Rodgers and Nicewander 1988):

$$R_{xy} = \frac{\sum (x_i - \bar{X}) \sum (y_i - \bar{Y})}{\sqrt{\sum (x_i - \bar{X})^2} \sqrt{\sum (y_i - \bar{Y})^2}}$$

10

where  $\bar{X}$  denotes the mean of  $x$ ,  $\bar{Y}$  denotes the mean of  $y$ .

Spatial correlation coefficients were calculated between the average annual VCI (dependent variable) and the annual accumulative PCI, yearly average TCI, yearly average SMCI and yearly average MIDI (independent variables) using Pearson correlation method (Zhou et al. 2016). The significance of the correlation coefficients was judged at the confidence of 95% level.

## 3. Results

### 3.1. Analysis of VC variations

Figure 4 shows the average intra-year vegetation coverage of the eastern basins in Afghanistan throughout the study period. The VC had a slightly decreasing trend from the first of January ( $\sim 12\%$  of study area covered in vegetation,  $19,662 \text{ km}^2$ ) until the 2 February ( $\sim 11\%$  of study area covered in vegetation,  $18,063 \text{ km}^2$ ). From 2 February to 25 March vegetation coverage increased from  $\sim 2-46\%$  of the study area ( $75,635 \text{ km}^2$ ). Then, from 25 March, it decreased from  $46-13\%$  of the study area on 19 December (about  $20679 \text{ km}^2$ ). The vegetation cover increase was very high from 25 March to 26 June, same as the decrease from 26 June to 17 November, whereas between 17 November and 19 December, it was relatively slow. From the above results, we can conclude that the peak of VC in the eastern basins of Afghanistan is observed in May and June.

Figure 5 presents the relationship between annual vegetation coverage and the annual mean of the area affected by drought conditions for the eastern basins of Afghanistan during the studied period (2000–

2021). The annual mean of the area affected by drought conditions was calculated using the percentage range value of the VCI index. If the value was between 0 and 50% it indicated that the area (pixel) under consideration had bad vegetation growth conditions and was affected by drought conditions (DAV), whereas values from 50.1 to 100% indicated good vegetation growth conditions, and that the area was not affected by drought conditions (NDAV). It is worth mentioning here that DAV can take larger values than VC because for the calculation of the area the values of  $NDVI < 0.2$  (barren land, rocks, buildup areas) are also taken into account. The maximum VC was observed for 2005, 2010, 2013, 2016 and 2020 (70%, 71%, 71%, 72% and 72% of the study area, with 113,894, 116,570, 116,718, 117,821 and 118,389  $km^2$ , respectively), while for 2000, 2001, and 2008 the minimum VC was recorded (56, 56, and 55% of the study area, with 91,747, 91,847, and 90,576  $km^2$ , respectively). The maximum DAV was observed in 2000 and 2001 (87 and 89% of the study area, 142,638 and 146,195  $km^2$ , respectively), whereas the minimum DAV was recorded in 2010, 2012, and 2020 (81, 82, and 82% of the study area, with 133,221, 134,110, and 134,016  $km^2$ , respectively). The relationship between VC and DAV assessed with the use of the linear regression model was significant at the 95% confidence level ( $R = 0.78$ ,  $p\text{-value} < 0.05$ ).

Figure 6 shows the maps of vegetation coverage in the eastern basins of Afghanistan for the years with the lowest (2000 and 2008) and the highest (2016 and 2020) vegetation coverage. Better vegetated areas were observed in the northern and northeastern areas of ADB and the eastern and southeastern areas of the KRB, whereas in the eastern, southeastern, and southwestern areas of the ADB, and the western and southwestern areas of the KRB vegetation occupied a much smaller area.

The areas with changes in vegetation are shown in red color (compared to the year with the highest vegetation during the studied period, which was 2020). It results from Fig. 2 that they are mostly seen in agricultural lands, what is probably connected with human activities.

## 3.2. Annual variations of MIDI

In Fig. 7 the maps of the spatial variations of MIDI in the eastern basins of Afghanistan are presented separately for each year from the studied period (2000–2021), whereas in Fig. 8 the same information is aggregated into a column plot for better comparison of temporal changes. In 2000, which can be recognized as the year affected by extreme and severe drought to the highest degree among the years analyzed, most of the studied area (32%, 51,968  $km^2$ ) was affected by severe drought conditions. Severe drought affected most of the southwestern and western areas of the KRB, and the northwestern and western areas of the ADB in the Kunduz sub-basin, while the extreme drought conditions were affecting some parts of the KRB in the Gomal sub-basin only (~ 1% of the study area, 1218  $km^2$ ). For most of the central and northeastern areas of these two basins (20% of the study area, 34,121  $km^2$ ), no drought conditions were observed. In 2001, most of the southwest and west areas of KBR, and northwest of ADB were affected by moderate drought (33% of the study area, 54,596  $km^2$ ). In 2002, areas without drought, mild drought, and moderate drought almost have the same size (27, 29, and 29% of the studied area, 44,778, 48,098, and 47,449  $km^2$ , respectively), and severe drought had affected very few areas of the

southwest KRB (6% of the study area, 9829 km<sup>2</sup>). In 2003, most of the central areas had no drought conditions (39% of the study area, 63,928 km<sup>2</sup>), however, some areas in the southwest of KRB and the northeast of the ADB had been affected by moderate drought (26% of the study area, 42,272 km<sup>2</sup>).

In 2004, most of the northern, northeastern, and central areas of the basins experienced no drought conditions (35% of the study area, 56,889 km<sup>2</sup>), in turn, the southwest areas of the KRB had been affected by severe drought (15% of the study area, 24,850 km<sup>2</sup>). 2009 was one of the years least affected by the effects of extreme, severe, and moderate drought conditions from the studied period, and also had the highest area that hadn't experienced drought (55% of the study area, 90,785 km<sup>2</sup>). Only some areas in the northeast and northwest of the ADB and the southwest of the KRB had been affected by mild, moderate, and severe drought (32, 7, and 2% of the study area, 52,499, 11,948, and 2474 km<sup>2</sup>, respectively). In 2011, most of the central northeast, and southeast areas of the basin were under mild drought conditions (39% of the study area, 63,939 km<sup>2</sup>), and the northwest areas of the ADB and the southwest areas of the KRB were under moderate drought (39% of the study area, 64,043 km<sup>2</sup>). In 2016, most of the northwestern and southwestern areas of the study area and some southern areas of the ADB were affected by moderate drought (35% of the study area, 57,937 km<sup>2</sup>), and most of the central and southwestern areas of the study area hadn't experienced drought (25% of the study area, 42,253 km<sup>2</sup>). 2019 and 2020 were the second and the third year of the studied period with the highest area that hadn't experienced drought. In 2019, 51% of the study area (83,682 km<sup>2</sup>) was under no drought conditions, except for some areas in the southwest of the KRB and the east of the ADB, which were affected by mild and moderate drought (12% and 40% of the study area, 20,650 and 65,654 km<sup>2</sup>, respectively). In 2020 only some areas in the southwest of the KRB and the south of the ADB were affected by mild and moderate drought (30% and 17% of the study area, 48,654 and 27,409 km<sup>2</sup>, respectively), while 48% of the study area (79,342 km<sup>2</sup>) was without drought conditions. From the temporal changes of meteorological drought in the eastern Basin of Afghanistan during the study period shown in Fig. 8, it results that the areas affected by extreme, severe, and moderate droughts had a downward trend, whereas the trends for the areas affected by mild drought, and with no drought conditions were upwards.

According to Fig. 7, severe meteorological drought has occurred in the northeastern, northwestern, and south parts of the ADB, and in the southwestern and southern areas of the KRB, almost in all of the studied years. Conversely, according to Fig. 6, these areas were either without vegetation cover or are covered by the vegetation to a small extent in 2000, 2008, 2016, and 2020.

### **3.3. Correlation of VC with other variables**

Figure 9 shows the annual anomalies of VC, precipitation, soil moisture, LST, and MIDI for the eastern basins of Afghanistan during 2000–2021. 2000, 2001, 2016, 2017, 2018, and 2021 were the years with the highest LST (22.3, 18.6, 18.8, 18, 18, and 18.4°C on average, respectively) during the study period. In turn, 2012, 2019, and 2020 had the lowest LSTs (15.2, 16.2, 16.6°C, respectively). 2009, 2012, 2013, 2014, and 2015 had the highest precipitation (525, 569, 574, 590, and 675 mm, respectively) during the study

period, whereas 2000, 2001, 2017, and 2021 had the lowest precipitation (211, 217, 330 and 269 mm, respectively). For 2005, 2009, 2012, 2015, and 2019 the highest soil moisture was recorded (23, 22, 24, and 23.4  $\text{m}^3\text{m}^{-3}$ , respectively) during the study period, and conversely, for 2001, 2002, 2008, and 2021 the lowest soil moisture was observed (17, 18, 19.4 and 18.6  $\text{m}^3\text{m}^{-3}$ , respectively). 2000, 2001, 2004 and 2008 had the lowest vegetation coverage (91,747, 91,847, 98,750, and 90,576  $\text{km}^2$ , respectively), while 2005, 2010, 2013, 2016 and 2020 were the greenest years with the highest vegetation coverage (113,894, 116,570, 116,718, and 118840  $\text{km}^2$ , respectively). Meteorological drought conditions calculated with the use of MIDI indicated that in 2000, 2001, 2010, 2011, and 2021 the most area had been affected by meteorological drought (133,049, 133,554, 145,906, 146,870, and 135,398  $\text{km}^2$ , respectively). In turn, in 2005, 2009, 2019 and 2020 the smallest area was affected by drought (91,950, 76,475, 83,511, and 87,939  $\text{km}^2$ , respectively). In 2005, precipitation was close to the normal value (precipitation Z-score was close to 0), LST and MIDI were below normal value, but the soil moisture and vegetation cover were above the normal value. Almost the same can be observed for 2020, in which the precipitation, MIDI, and LST were below the normal value, but the soil moisture and vegetation coverage were above the normal value. It strongly suggests that soil moisture was one of the key parameters controlling the LST and had the highest impact on the variations in the vegetation coverage. The decrease in the annual mean LST for the eastern basins of Afghanistan in the studied period was  $-0.06^\circ\text{C}$ , while an increase in the annual mean precipitation was 6.9 mm yearly. Annual mean soil moisture also had an increasing trend, whereas the area with meteorological drought had a decreasing trend during the study period.

Figure 10 and Table 3 show the relationship between the annual mean of the vegetation cover and assessed meteorological parameters, such as precipitation, soil moisture, drought-affected area calculated on the base of MIDI (MIDI area), and LST for the studied period. A positive relationship was observed for VC and precipitation, and VC and soil moisture, whereas a negative relationship was seen for VC and LST, and VC and MIDI area. It was found that the relationships between VC and precipitation, VC and soil moisture, and VC and LST were significant ( $R = 0.64$ ,  $p = 0.008$ ;  $R = 0.73$ ,  $p = 0.0004$ ; and  $R = 0.57$ ,  $p = 0.04$ , respectively), whereas the relationship between VC and MIDI area was not significant ( $R = 0.36$ ,  $p = 0.126$ ) at the 95% confidence level.



Table 3

The correlation ( $R$ ) and determination ( $R^2$ ) coefficients and  $p$ -value for relationships between annual vegetation coverage and precipitation, soil moisture, LST, and MIDI for the eastern basins of Afghanistan during 2000–2021 calculated using the linear regression method.

	$R$	$R^2$	$p$ -value
Vegetation coverage – Precipitation	0.64*	0.41	0.008
Vegetation coverage – Soil moisture	0.73*	0.53	0.0004
Vegetation coverage – LST	0.57*	0.33	0.04
Vegetation coverage – MIDI area	0.36	0.13	0.126

\* denotes that the correlation was significant ( $p$ -value = 0.05).

Table 4

The yearly multiple regression relationships between vegetation coverage, precipitation, soil moisture (SM), and LST for the eastern basins of Afghanistan during 2000–2021.

Model of vegetation coverage	$R$ (Regression coefficient)	$R^2$ (Determination coefficient)	Multiple regression equations
yearly	0.74	0.45	$VC_{\text{yearly}} = 5.17 - 0.00029 \cdot \text{Precipitation}_{\text{yearly}} + 0.352 \cdot \text{SM}_{\text{yearly}} - 0.137 \cdot \text{LST}_{\text{yearly}} + 0.066 \cdot \text{MIDI}_{\text{yearly}}$

For the variations of VC, the multiple regression equations taking into account the relationships between VC, precipitation, soil moisture, LST, and MIDI area for the eastern basins of Afghanistan during 2000–2021 were calculated for the yearly values (Table 4). These equations allow estimating the projected value of VC. The obtained multiple regression and determination coefficients indicate that precipitation, soil moisture, and LST explained about 45% of the yearly VC variations.

### 3.4. Spatial variability of the analyzed variables in the period 2000–2021

In Fig. 11 the spatial variations in the mean precipitation, LST, soil moisture, vegetation cover, and meteorological drought index for the period of 2000–2021 are presented. The highest precipitation occurred in the flat areas of north, northeast, south, and southeast of the KRB area and the north, south, and central areas of the ADB, The smallest amounts of precipitation were observed for the areas with high altitudes. Generally, the yearly precipitation sums in these basins increased during the study period. In the southern, southeastern, and southwestern areas of the KRB and the western, northwestern, and southwestern areas of the ADB, LST was high. Generally, the LST decreased in the study area during the study period. LST had an inverse relationship with the orography (Table 5), as, for example, it could be observed for the part of Wakhan district of Badakhshan province, which has high elevation and low LST. Soil moisture depended mostly on the amount of rainfall in the area.

Table 5

The correlation ( $R$ ) and determination ( $R^2$ ) coefficients and  $p$ -value for relationships between elevation and PCI, SMCI, TCI, and MIDI for the eastern basins of Afghanistan calculated using the linear regression method.

	$R$	$R^2$	$p$ -value
Elevation – PCI	0.036*	0.001	0.04
Elevation – TCI	0.9*	0.8	0
Elevation – SMCI	0.019*	0.03	0
Elevation – MIDI	0.38*	0.14	0
Elevation – VCI	0.6*	0.3	0

The correlation coefficients ( $R$ ) between the mean VCI, and the mean PCI, TCI, SMCI, and MIDI were calculated to determine the relationship between vegetation conditions and climatic variables. The correlations between VCI and precipitation, temperature, soil moisture, and drought, presented in Fig. 12, were dependent on the orography. In the majority of flat areas, the correlation between VCI and PCI index was positive, whereas in mountainous areas negative correlations were observed. The correlation between the TCI index and VCI was negative in mountainous areas and positive in some flat areas. The correlation between VCI and SMCI index was positive in most flat and low-altitude areas and negative in some mountainous areas. The correlation between the VCI index and MIDI in most of the areas with vegetation was negative, whereas for the areas with a lack of vegetation it was positive.

## 4. Discussion

While Afghanistan's natural ecosystems have already been destroyed during the country's many years of civil wars, unsustainable management, and over-exploitation, literature reports indicate that Afghanistan will face a wide range of new and increased climate risks (Kimura 2020). The worst adverse effects of

climate change on Afghanistan are related to drought, including these leading to desertification and land degradation. Severe drought conditions occurring for prolonged periods can lead to aridification in drought-affected regions (Ma and Fu 2007). Drought is estimated to be the norm by 2030, not a periodic event (Kimura 2020). Currently, Afghanistan is facing significant drought issues that have a direct impact on livelihoods and the economy. The drought that occurred in 2011 has pushed millions of people into food insecurity and poverty (Ranghieri et al. 2017). Although few studies have determined the impact of drought events, there is still a need to assess its impact on various aspects, like vegetation coverage dynamic, especially for longer periods.

In this study, the relationship between vegetation coverage dynamic and meteorological parameters (precipitation, soil moisture, and LST) and meteorological drought conditions was assessed for the eastern basins of Afghanistan for the period 2000–2021. Despite the climate changes that are occurring in Afghanistan (Rousta et al. 2020a), the average annual vegetation coverage increased in the eastern basins of Afghanistan in the study period. A significant increase in VC from 2000 to 2003 was observed, after that, from 2005 to 2008, a slight decrease happened. 2008 had the minimum VC (55% of the study area), and since 2009, VC had increased (except for 2011) since 2016. Although a decreasing trend was observed from 2016 until 2018, after that, from 2018 to the end of the assessed period, there was a slight upward trend in the vegetation coverage. A strong and significant correlation between the annual mean of VC and the area affected by drought conditions expressed with the use of VCI (the values of the VCI = < 50%) was found ( $R = 0.78$ ,  $p = 0.000014$ ). Obtained results were in line with other research made for the whole Afghanistan territory (Rousta et al. 2020a), in which it was found that the vegetation coverage was increasing in the period 2001–2018. The authors found that the correlation between NDVI and VCI was high, whereas the correlation between NDVI and LST was low. Additionally, it was stated that in 2000 and 2008 the lowest vegetation coverage was observed, while in 2010 and 2016 the highest vegetation coverage was recorded.

In general, the area with meteorological drought conditions ( $MIDI = < 0.4$ ) had a decreasing trend in the study period. The area decreased from 2000 to 2005, and then it increased from 2005 to 2007. Similarly, from 2010 to 2020 a downward trend was observed for the area with meteorological drought conditions. The areas under extreme, severe, and moderate meteorological drought were decreasing, while the area with mild drought conditions was increasing during the study period. Most areas were affected by moderate and mild droughts. These results were in line with the other research made for the Kabul river basin (Baig et al. 2020), in which it was stated that 2000 and 2004 were the years with the worst meteorological drought conditions from the period from 2000 to 2018 and that the trend of meteorological drought changes in KRB was downward. During the studied period most of the northwest, southwest and some eastern areas of the eastern basins in Afghanistan had been influenced by drought. The highest value of the area under meteorological drought was observed in 2000, 2001, 2007, 2010, 2011, and 2021 (81, 82, 85, 90, and 83% of the study area affected by drought, respectively).

Observed variations in annual VC were related to the changes in meteorological parameters. For example, in 2000 and 2021 annual VC was below normal value, simultaneously with annual precipitation, and soil

moisture, whereas LST was above the normal value. In 2015 and 2019, annual VC was above normal value, simultaneously with annual precipitation, and soil moisture, whereas annual LST was below the normal value. Obtained results indicated that the correlation between VC and precipitation was positive and significant ( $R = 0.64$ ,  $p = 0.008$ ), and the total annual precipitation had an upward trend during the study period (Yu et al. 2020). The correlation between VC and soil moisture was positive and significant ( $R = 0.73$ ,  $p = 0.0004$ ), and the annual mean soil moisture had an upward trend during the study period (Pei et al. 2018). The correlation between VC and LST was also positive and significant ( $R = 0.57$ ,  $p = 0.04$ ), and the annual mean LST was decreasing during the study period. The correlation between VC and metrological drought was not significant ( $R = 0.36$ ,  $p = 0.126$ ) at a 95% confidence level. Obtained results are somewhat in line with the other research made for Kabul River Basin in Afghanistan (Rousta et al. 2022b), in which the vegetation coverage dynamics and its relation to atmospheric patterns were investigated (Quan et al. 2022). It was found that the vegetation dynamics in KRB was impacted by both precipitation and LST, however, the magnitude of this impact depended on the season. During the winter LST had a greater impact on VC variation than precipitation, and conversely, in summer, precipitation impacted vegetation to a higher degree than LST. In another study, the vegetation dynamics and its relationship with climatological factors for Caspian Sea watersheds in Iran was analyzed (Rousta et al. 2022a). It was found that the correlations of vegetation coverage with ET and LST in winter were positive and significant ( $R = 0.46$  and  $0.55$ ,  $p$ -value =  $0.05$ , respectively), while the correlation with the precipitation was not significant. In the spring, the correlation between VC and precipitation was positive and significant ( $R = 0.55$ ,  $p$ -value =  $0.05$ ), but the impact of LST on the vegetation coverage was negligible when the precipitation was abnormally high. In the summer, the correlation between VC and LST was negative and significant ( $R = -0.45$ ,  $p$ -value =  $0.05$ ).

## 5. Conclusions

In the present study, the impact of meteorological parameters and meteorological drought on the vegetation coverage in the eastern basins of Afghanistan has been investigated using remote sensing data. It was found that soil moisture had a high impact on VC, and the LST impacted VC to the slightest extent from the studied meteorological parameters. The relationship between VC and the area under meteorological drought was insignificant. The correlations between VC and precipitation, soil moisture, and LST were positive and significant ( $R = 0.64$ ,  $p = 0.008$ ,  $R = 0.73$ ,  $p = 0.0004$ ,  $R = 0.57$ ,  $p = 0.04$ , respectively). It was revealed that precipitation, soil moisture, LST, and area under meteorological drought conditions explained about 45% of the yearly VC variation in the eastern basins of Afghanistan.

The results of this research indicated that the changes in the vegetation coverage in the eastern basins of Afghanistan during 2000–2021 had an upward trend. VC increased slightly from 2000 to 2005 and decreased slightly from 2005 to 2008, with 2008 being the year with the least vegetation during the studied period. From 2008 to 2021, VC generally increased, however, a slight downward trend was observed between 2016 and 2018. Annual mean LST had a downward trend, whereas total annual precipitation had an upward trend during the study period. In most parts of Afghanistan, the vegetation

depends on the winter rain, however, in the south winter rains are often irregular. Rainfall increases to the north and east resulting in better vegetation conditions in these parts. The eastern parts additionally receive some monsoon rains in summer (Breckle 2007). Annual mean soil moisture had an upward trend, and the areas under extreme, severe, and moderate meteorological drought conditions were declining during the studied period. In turn, the areas with mild meteorological drought conditions had an upward trend in the study period.

## Declarations

**Author Contributions:** A.F.N. and I.R. proposed the topic. A.F.N., I.R., G.M., M.D., and H.O. commanded the data processing and analysis. A.F.N., I.R., G.M., M.D., H.O., A.S., and J.K. wrote the manuscript. J.K., A.S., P.T., and P.B. enhanced the research design, helped to analyze and interpret the results, and revised the manuscript. All authors have read and agreed to the published version of the manuscript.

**Funding:** This research was supported by Vedurfelagid, Rannis and Rannsoknastofa i vedurfraedi.

**Acknowledgments:** Iman Rousta is deeply grateful to his supervisor (Haraldur Olafsson, Professor of Atmospheric Sciences, Institute for Atmospheric Sciences-Weather and Climate, and Department of Physics, University of Iceland, and Icelandic Meteorological Office (IMO)), for his great support, kind guidance, and encouragement.

**Institutional Review Board Statement:** Not applicable.

**Informed Consent Statement:** Not applicable.

**Data Availability Statement:** Not applicable.

**Conflicts of Interest:** The authors declare no conflict of interest. The funders had no role in the design of the study; in the collection, analyses, or interpretation of data; in the writing of the manuscript, or in the decision to publish the results.

## References

1. Aich V et al. (2017) Climate change in Afghanistan deduced from reanalysis and coordinated regional climate downscaling experiment (CORDEX)—South Asia simulations *Climate* 5:38
2. Akhtar F, Awan UK, Tischbein B, Liaqat UW (2018) Assessment of irrigation performance in large river basins under data scarce environment—A case of Kabul river basin, Afghanistan *Remote Sensing* 10:972
3. Akhundzadah NA, Soltani S, Aich V (2020) Impacts of climate change on the water resources of the Kunduz River Basin, Afghanistan *Climate* 8:102
4. Ali S, Tong D, Xu ZT, Henchiri M, Wilson K, Siqi S, Zhang J (2019) Characterization of drought monitoring events through MODIS-and TRMM-based DSI and TVDI over South Asia during 2001–

5. Baig MHA, Abid M, Khan MR, Jiao W, Amin M, Adnan S (2020) Assessing meteorological and agricultural drought in Chitral Kabul river basin using multiple drought indices Remote Sensing 12:1417
6. Bi H, Ma J, Zheng W, Zeng J (2016) Comparison of soil moisture in GLDAS model simulations and in situ observations over the Tibetan Plateau Journal of Geophysical Research: Atmospheres 121:2658-2678
7. Borgogno-Mondino E, Lessio A, Gomarasca MA (2016) A fast operative method for NDVI uncertainty estimation and its role in vegetation analysis European Journal of Remote Sensing 49:137-156
8. Breckle S-W (2007) Flora and vegetation of Afghanistan Basic and Applied Dryland Research 1:155-194
9. Cesaro J-D, Jolivot A, Taugourdeau S (2019) Mapping Amu Darya's ecosystem riverbanks: land cover, ecology and LABR management
10. Chen Z, Liu Z, Yin L, Zheng W (2022) Statistical analysis of regional air temperature characteristics before and after dam construction Urban Climate 41:101085
11. Du L, Tian Q, Yu T, Meng Q, Jancso T, Udvardy P, Huang Y (2013) A comprehensive drought monitoring method integrating MODIS and TRMM data International Journal of Applied Earth Observation and Geoinformation 23:245-253
12. Gao C, Hao M, Chen J, Gu C (2021) Simulation and design of joint distribution of rainfall and tide level in Wuchengxiyu Region, China Urban Climate 40:101005
13. Gao Y, Huang J, Li S, Li S (2012) Spatial pattern of non-stationarity and scale-dependent relationships between NDVI and climatic factors—A case study in Qinghai-Tibet Plateau, China Ecological Indicators 20:170-176
14. Gascon M, Cirach M, Martínez D, Dadvand P, Valentín A, Plasència A, Nieuwenhuijsen MJ (2016) Normalized difference vegetation index (NDVI) as a marker of surrounding greenness in epidemiological studies: The case of Barcelona city Urban Forestry & Urban Greening 19:88-94
15. Han Y et al. (2020) Monitoring droughts in the Greater Changbai Mountains using multiple remote sensing-based drought indices Remote Sensing 12:530
16. Hu S, Wu H, Liang X, Xiao C, Zhao Q, Cao Y, Han X (2022) A preliminary study on the eco-environmental geological issue of in-situ oil shale mining by a physical model Chemosphere 287:131987
17. Huang S, Tang L, Hupy JP, Wang Y, Shao G (2021a) A commentary review on the use of normalized difference vegetation index (NDVI) in the era of popular remote sensing Journal of Forestry Research 32:1-6
18. Huang W, Duan W, Chen Y (2021b) Rapidly declining surface and terrestrial water resources in Central Asia driven by socio-economic and climatic changes Science of The Total Environment 784:147193

19. Huffman GJ, Bolvin DT, Braithwaite D, Hsu K, Joyce R, Xie P, Yoo S-H (2015) NASA global precipitation measurement (GPM) integrated multi-satellite retrievals for GPM (IMERG) Algorithm Theoretical Basis Document (ATBD) Version 4
20. Jawadi HA, Malistani HA, Mohamdi H Climate Change and Variability Effects on Water supplies, Hazards, Land degradation and Migration in Afghanistan (with examples from Central Highlands)
21. Ji L, Peters AJ (2005) Lag and seasonality considerations in evaluating AVHRR NDVI response to precipitation *Photogrammetric Engineering & Remote Sensing* 71:1053-1061
22. Karnieli A, Bayasgalan M, Bayarjargal Y, Agam N, Khudulmur S, Tucker C (2006) Comments on the use of the vegetation health index over Mongolia *International Journal of Remote Sensing* 27:2017-2024
23. Kimura R (2020) Global detection of aridification or increasing wetness in arid regions from 2001 to 2013 *Natural Hazards* 103:2261-2276
24. Klemm W, Shobair S (2010) The Afghan part of Amu Darya basin. Impact of irrigation in Northern Afghanistan on water use in the Amu Darya basin Food and Agriculture Organization
25. Lee Rodgers J, Nicewander WA (1988) Thirteen ways to look at the correlation coefficient *The American Statistician* 42:59-66
26. Leprieur C, Kerr Y, Mastorchio S, Meunier J (2000) Monitoring vegetation cover across semi-arid regions: comparison of remote observations from various scales *International Journal of Remote Sensing* 21:281-300
27. Li J, Charles LS, Yang Z, Du G, Fu S (2022a) Differential Mechanisms Drive Species Loss Under Artificial Shade and Fertilization in the Alpine Meadow of the Tibetan Plateau *Frontiers in plant science* 13:832473-832473
28. Li W et al. (2021) Fine root biomass and morphology in a temperate forest are influenced more by the nitrogen treatment approach than the rate *Ecological Indicators* 130:108031
29. Li X, Wang Y, Hu Y, Zhou C, Zhang H (2022b) Numerical investigation on stratum and surface deformation in underground phosphorite mining under different mining methods *Frontiers in Earth Science* 10
30. Li Z, Kafatos M (2000) Interannual variability of vegetation in the United States and its relation to El Nino/Southern Oscillation *Remote sensing of environment* 71:239-247
31. Liu S, Liu Y, Wang C, Dang X (2022) The Distribution Characteristics and Human Health Risks of High-Fluorine Groundwater in Coastal Plain: A Case Study in Southern Laizhou Bay, China *Frontiers in Environmental Science*:568
32. Liu W, Kogan F (1996) Monitoring regional drought using the vegetation condition index *International Journal of Remote Sensing* 17:2761-2782
33. Liu Y, Zhang K, Li Z, Liu Z, Wang J, Huang P (2020) A hybrid runoff generation modelling framework based on spatial combination of three runoff generation schemes for semi-humid and semi-arid watersheds *Journal of Hydrology* 590:125440

34. Loveland TR, Zhu Z, Ohlen DO, Brown JF, Reed BC, Yang L (1999) An analysis of the IGBP global land-cover characterization process Photogrammetric engineering and remote sensing 65:1021-1032
35. Ma Z, Fu C (2007) Global aridification in the second half of the 20th century and its relationship to large-scale climate background Science in China Series D: Earth Sciences 50:776-788
36. Maharjan SB, Shrestha F, Azizi F, Joya E, Bajracharya B, Bromand MT, Rahimi MM (2021) Monitoring of Glaciers and Glacial Lakes in Afghanistan. In: Earth Observation Science and Applications for Risk Reduction and Enhanced Resilience in Hindu Kush Himalaya Region. Springer, Cham, pp 211-230
37. Mahmood SAR, Rousta I, Mazidi A (2022) Investigating the Sustainability of Vegetation Change Trends Using Remote Sensing (Case Study: Northern River Basin of Afghanistan) Geography and Environmental Sustainability 12:17-35
38. Mansourmoghaddam M, Ghafarian Malamiri HR, Arabi Aliabad F, Fallah Tafti M, Haghani M, Shojaei S (2022a) The Separation of the Unpaved Roads and Prioritization of Paving These Roads Using UAV Images Air, Soil and Water Research 15:11786221221086285
39. Mansourmoghaddam M, Ghafarian Malamiri HR, Rousta I, Olafsson H, Zhang H (2022b) Assessment of Palm Jumeirah Island's Construction Effects on the Surrounding Water Quality and Surface Temperatures during 2001–2020 Water 14:634
40. Mansourmoghaddam M, Naghipur N, Rousta I, Ghaffarian HR (2022c) Temporal and Spatial Monitoring and Forecasting of Suspended Dust Using Google Earth Engine and Remote Sensing Data (Case Study: Qazvin Province) Desert Management 10:77-98
41. Mansourmoghaddam M, Rousta I, Zamani M, Mokhtari MH, Karimi Firozjaei M, Alavipanah SK (2022d) Study and prediction of land surface temperature changes of Yazd city: assessing the proximity and changes of land cover Journal of RS and GIS for Natural Resources 12:1-5
42. Mansourmoghaddam M, Rousta I, Zamani MS, Mokhtari MH, Karimi Firozjaei M, Alavipanah SK (2022e) Investigating And Modeling the Effect of The Composition and Arrangement of The Landscapes of Yazd City on The Land Surface Temperature Using Machine Learning and Landsat-8 and Sentinel-2 Data Iranian Journal of Remote Sensing & GIS
43. McNally A et al. (2017) A land data assimilation system for sub-Saharan Africa food and water security applications Scientific data 4:1-19
44. Munyasya AN et al. (2022) Integrated on-site & off-site rainwater-harvesting system boosts rainfed maize production for better adaptation to climate change Agricultural Water Management 269:107672
45. Najmuddin O, Deng X, Bhattacharya R (2018) The dynamics of land use/cover and the statistical assessment of cropland change drivers in the Kabul River Basin, Afghanistan Sustainability 10:423
46. Najmuddin O, Deng X, Siqi J (2017) Scenario analysis of land use change in Kabul River Basin—a river basin with rapid socio-economic changes in Afghanistan Physics and Chemistry of the Earth, Parts a/B/C 101:121-136



47. Omerkhil N, Chand T, Valente D, Alatalo JM, Pandey R (2020) Climate change vulnerability and adaptation strategies for smallholder farmers in Yangi Qala District, Takhar, Afghanistan *Ecological Indicators* 110:105863
48. Pei F et al. (2018) Monitoring the vegetation activity in China using vegetation health indices *Agricultural and forest meteorology* 248:215-227
49. Quan Q, Gao S, Shang Y, Wang B (2021) Assessment of the sustainability of *Gymnocypris eckloni* habitat under river damming in the source region of the Yellow River *Science of the Total Environment* 778:146312
50. Quan Q, Liang W, Yan D, Lei J (2022) Influences of joint action of natural and social factors on atmospheric process of hydrological cycle in Inner Mongolia, China *Urban Climate* 41:101043
51. Ranghieri F, Fallesen DMG, Jongman B, Balog-Way SAB, Mashahid SS, Siercke GA, Simpson AL (2017) Disaster risk profile: Afghanistan. The World Bank,
52. Rousta I, Mansourmoghaddam M, Olafsson H, Krzyszczyk J, Baranowski P, Zhang H, Tkaczyk P (2022a) Analysis of the recent trends in vegetation dynamics and its relationship with climatological factors using remote sensing data for Caspian Sea watersheds in Iran *International Agrophysics* 36:139-153
53. Rousta I et al. (2022b) Investigation of the Vegetation Coverage Dynamics and its Relation to Atmospheric Patterns in Kabul River Basin in Afghanistan *Pure and Applied Geophysics*:1-20
54. Rousta I, Olafsson H, Moniruzzaman M, Zhang H, Liou Y-A, Mushore TD, Gupta A (2020a) Impacts of drought on vegetation assessed by vegetation indices and meteorological factors in Afghanistan *Remote Sensing* 12:2433
55. Rousta I, Saberi M-a, Mahmood SA-r, Moghaddam MM, Olafsson H, Krzyszczyk J, Baranowski P (2020b) Climate Change impacts on vegetation and agricultural drought in the basin of Panjshir River in Afghanistan *Climate Change Research* 1:77-88
56. Sha S, Guo N, Li Y, Ren Y, Li Y (2013) Comparison of the vegetation condition index with meteorological drought indices: A case study in Henan province *Journal of Glaciology and Geocryology* 35:990-998
57. Shroder JF (2014) Natural resources in Afghanistan: geographic and geologic perspectives on centuries of conflict. Elsevier,
58. Testa S, Mondino ECB, Pedrolì C (2014) Correcting MODIS 16-day composite NDVI time-series with actual acquisition dates *European Journal of Remote Sensing* 47:285-305
59. Tian H, Qin Y, Niu Z, Wang L, Ge S (2021a) Summer Maize Mapping by Compositing Time Series Sentinel-1A Imagery Based on Crop Growth Cycles *Journal of the Indian Society of Remote Sensing* 49:2863-2874
60. Tian H, Wang Y, Chen T, Zhang L, Qin Y (2021b) Early-Season Mapping of Winter Crops Using Sentinel-2 Optical Imagery *Remote Sensing* 13:3822
61. Wang K, Li T, Wei J (2019) Exploring drought conditions in the three river headwaters region from 2002 to 2011 using multiple drought indices *Water* 11:190

62. Wang S et al. (2021) Exploring the utility of radar and satellite-sensed precipitation and their dynamic bias correction for integrated prediction of flood and landslide hazards *Journal of Hydrology* 603:126964
63. Wei W, Zhang J, Zhou L, Xie B, Zhou J, Li C (2021) Comparative evaluation of drought indices for monitoring drought based on remote sensing data *Environmental Science and Pollution Research* 28:20408-20425
64. Wu Y, Onipchenko V (2007) The impact of snow-cover on alpine vegetation type of different aspects in the west of Sichuan Province *Shengtai Xuebao* 27:5120-5129
65. Xie W, Li X, Jian W, Yang Y, Liu H, Robledo LF, Nie W (2021a) A novel hybrid method for landslide susceptibility mapping-based geodetector and machine learning cluster: A case of Xiaojin county, China *ISPRS International Journal of Geo-Information* 10:93
66. Xie W, Nie W, Saffari P, Robledo LF, Descote P-Y, Jian W (2021b) Landslide hazard assessment based on Bayesian optimization–support vector machine in Nanping City, China *Natural Hazards* 109:931-948
67. Xu J, Wu Z, Chen H, Shao L, Zhou X, Wang S (2022a) Influence of dry-wet cycles on the strength behavior of basalt-fiber reinforced loess *Engineering Geology* 302:106645
68. Xu J, Zhou L, Hu K, Li Y, Zhou X, Wang S (2022b) Influence of wet-dry cycles on uniaxial compression behavior of fissured loess disturbed by vibratory loads *KSCE Journal of Civil Engineering* 26:2139-2152
69. Yang Y et al. (2022) Increasing contribution of microbial residues to soil organic carbon in grassland restoration chronosequence *Soil Biology and Biochemistry* 170:108688
70. Yin L, Wang L, Keim BD, Konsoer K, Zheng W (2022a) Wavelet analysis of dam injection and discharge in three gorges dam and reservoir with precipitation and river discharge *Water* 14:567
71. Yin L et al. (2022b) Evaluation of empirical atmospheric models using Swarm-C satellite data *Atmosphere* 13:294
72. Yu H, Bian Z, Mu S, Yuan J, Chen F (2020) Effects of climate change on land cover change and vegetation dynamics in Xinjiang, China *International Journal of Environmental Research and Public Health* 17:4865
73. Zhang A, Jia G, Wang H (2019a) Improving meteorological drought monitoring capability over tropical and subtropical water-limited ecosystems: Evaluation and ensemble of the Microwave Integrated Drought Index *Environmental Research Letters* 14:044025
74. Zhang K et al. (2019b) The sensitivity of North American terrestrial carbon fluxes to spatial and temporal variation in soil moisture: An analysis using radar-derived estimates of root-zone soil moisture *Journal of Geophysical Research: Biogeosciences* 124:3208-3231
75. Zhang K, Shalehy MH, Ezaz GT, Chakraborty A, Mohib KM, Liu L (2022) An integrated flood risk assessment approach based on coupled hydrological-hydraulic modeling and bottom-up hazard vulnerability analysis *Environmental Modelling & Software* 148:105279

76. Zhang K, Wang S, Bao H, Zhao X (2019c) Characteristics and influencing factors of rainfall-induced landslide and debris flow hazards in Shaanxi Province, China *Natural hazards and earth system sciences* 19:93-105
77. Zhao T et al. (2021) Retrievals of soil moisture and vegetation optical depth using a multi-channel collaborative algorithm *Remote Sensing of Environment* 257:112321
78. Zhao T et al. (2020) Soil moisture experiment in the Luan River supporting new satellite mission opportunities *Remote Sensing of Environment* 240:111680
79. Zhao W, He J, Wu Y, Xiong D, Wen F, Li A (2019) An analysis of land surface temperature trends in the central Himalayan region based on MODIS products *Remote Sensing* 11:900
80. Zhao X, Xia H, Liu B, Jiao W (2022a) Spatiotemporal Comparison of Drought in Shaanxi–Gansu–Ningxia from 2003 to 2020 Using Various Drought Indices in Google Earth Engine *Remote Sensing* 14:1570
81. Zhao Z-Y et al. (2022b) Environmental risk of multi-year polythene film mulching and its green solution in arid irrigation region *Journal of Hazardous Materials* 435:128981
82. Zhongming W, Lees BG, Feng J, Wanning L, Haijing S (2010) Stratified vegetation cover index: A new way to assess vegetation impact on soil erosion *Catena* 83:87-93
83. Zhou G, Long S, Xu J, Zhou X, Song B, Deng R, Wang C (2021) Comparison analysis of five waveform decomposition algorithms for the airborne LiDAR echo signal *IEEE Journal of Selected Topics in Applied Earth Observations and Remote Sensing* 14:7869-7880
84. Zhou H, Deng Z, Xia Y, Fu M (2016) A new sampling method in particle filter based on Pearson correlation coefficient *Neurocomputing* 216:208-215
85. Zhu B, Zhong Q, Chen Y, Liao S, Li Z, Shi K, Sotelo MA (2022) A Novel Reconstruction Method for Temperature Distribution Measurement Based on Ultrasonic Tomography *IEEE Transactions on Ultrasonics, Ferroelectrics, and Frequency Control*

## Figures

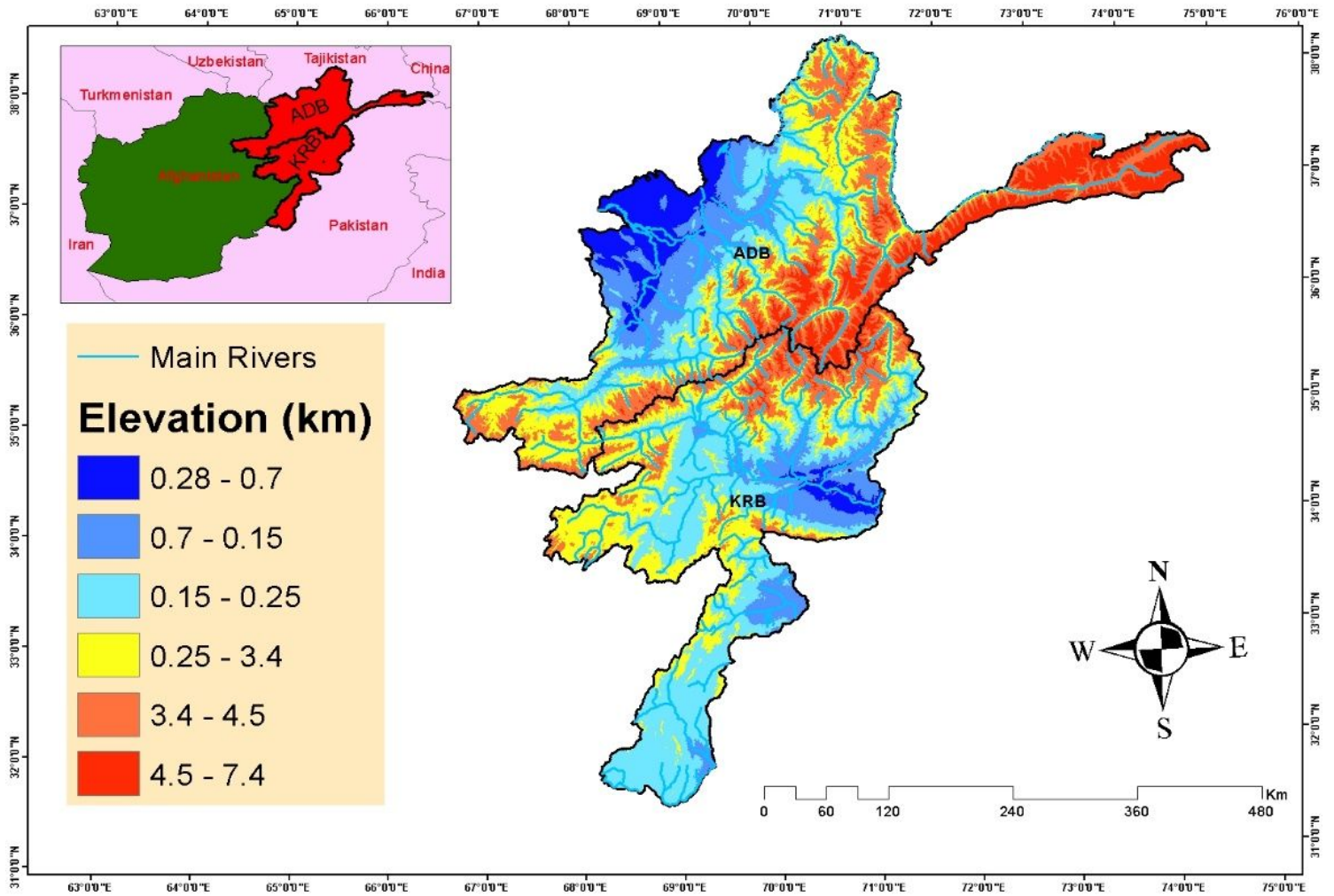


**Figure 1**

The map presenting elevation profile of Kabul River Basin and Amu Darya Basin in Afghanistan.

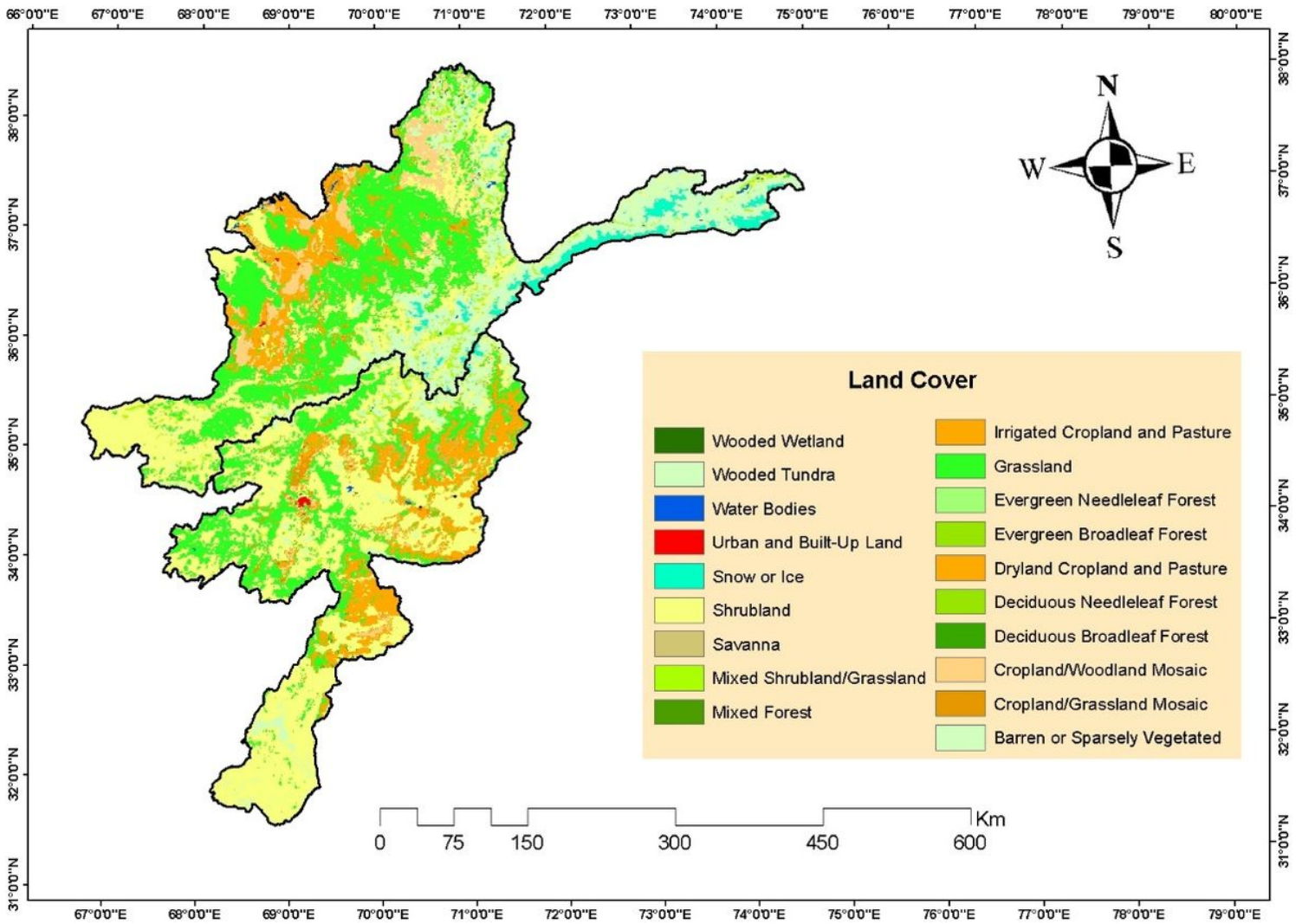


**Figure 2**

*Land cover types for Kabul River Basin and Amu Darya Basin of Afghanistan retrieved from MODIS (MCD12Q1) image from 2016.*

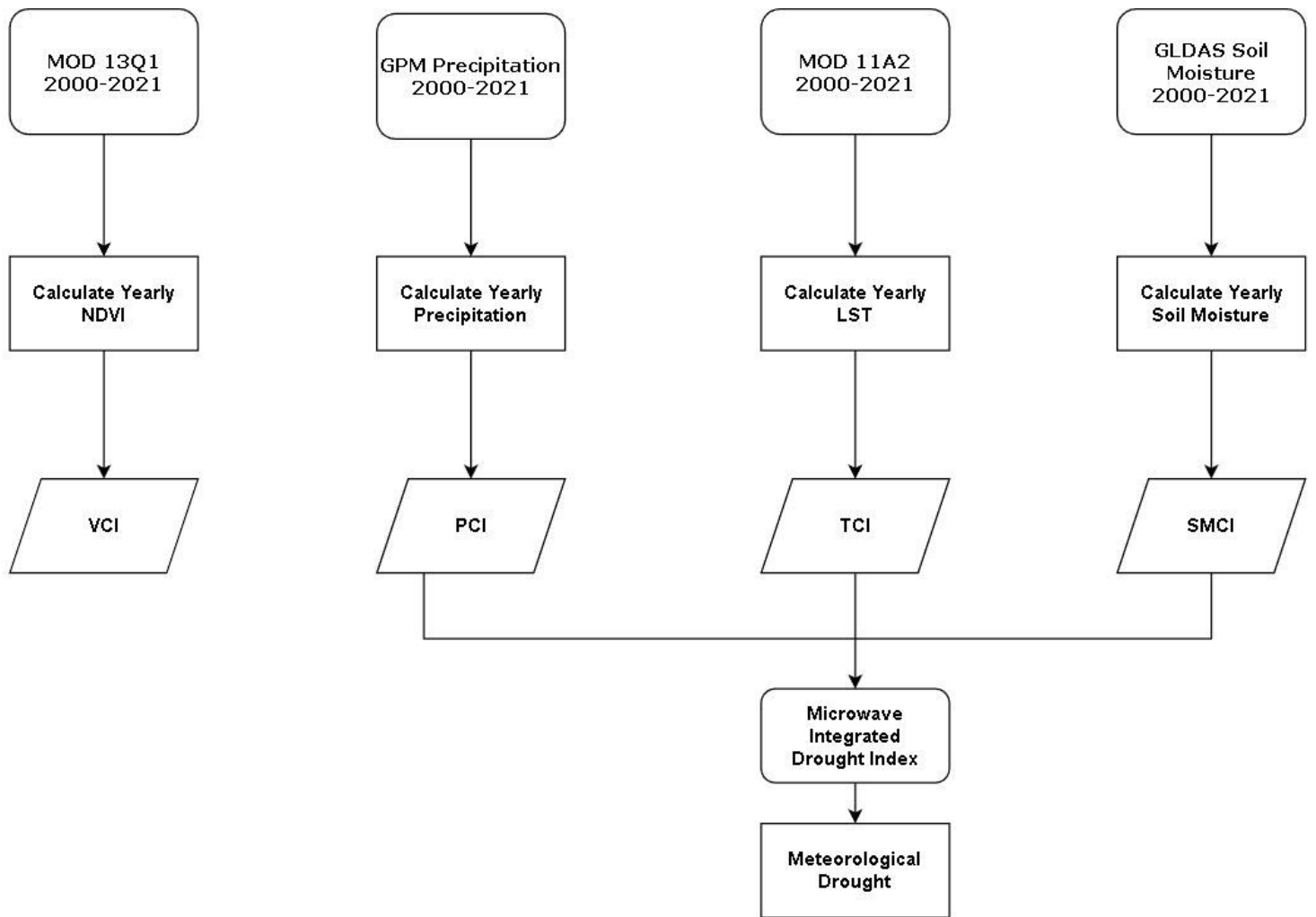


**Figure 3**

Flowchart of the data processing.

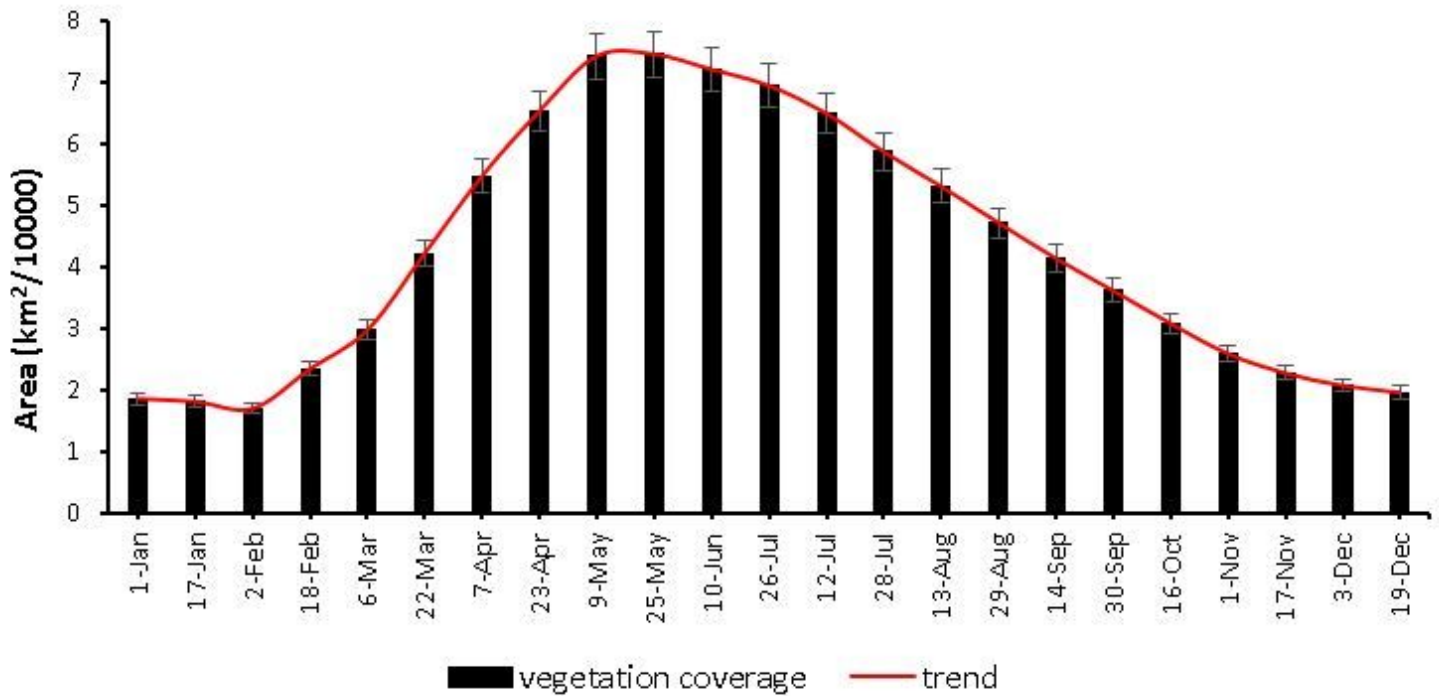


Figure 4

The average intra-year vegetation coverage of the eastern basins in Afghanistan during 2000-2021.

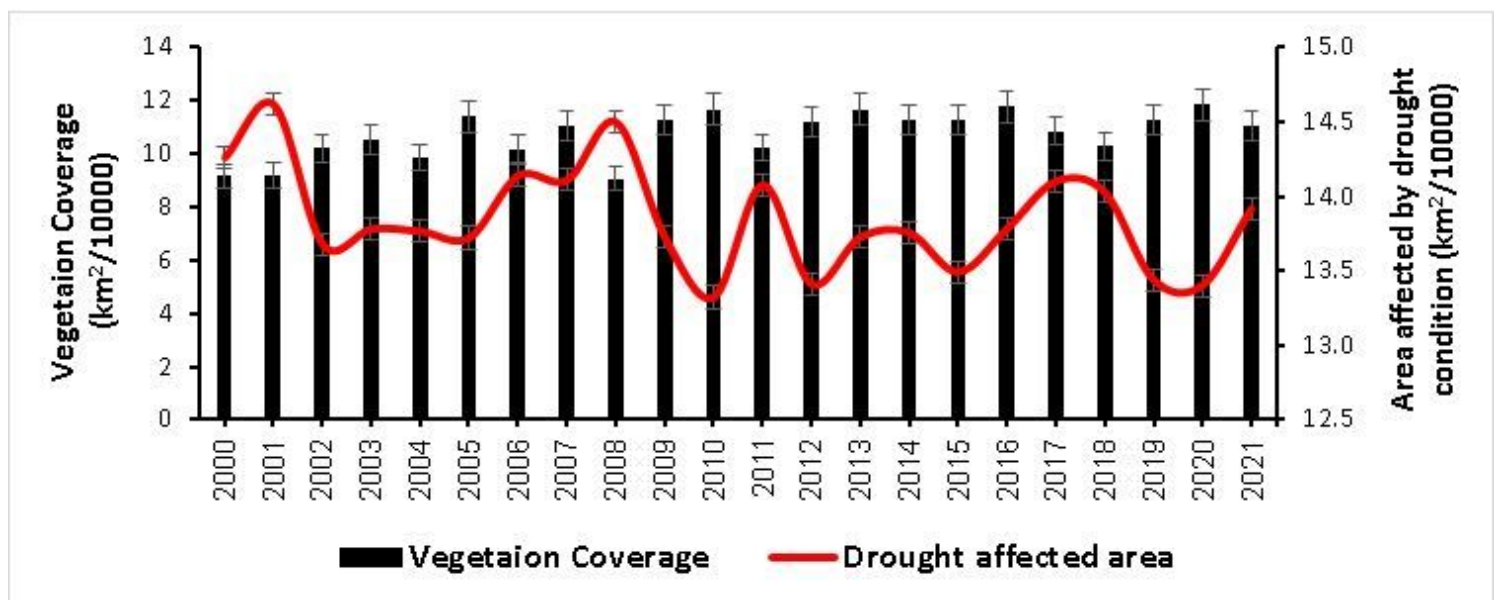
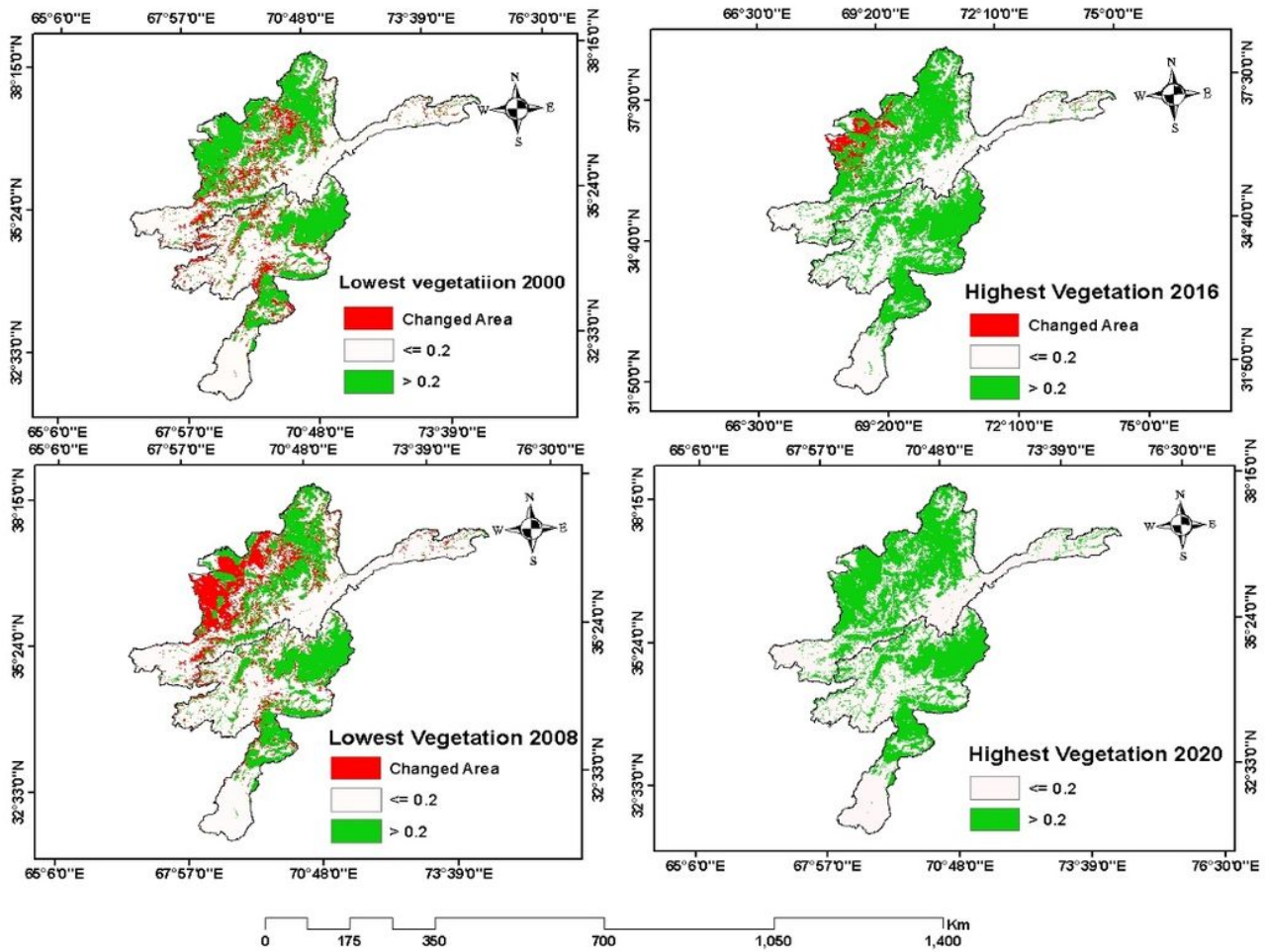


Figure 5

The average annual vegetation coverage (black bars) and average annual area affected by drought conditions (red line) of the eastern basins in Afghanistan during 2000-2021.





**Figure 6**

The maps of annual means of NDVI for the eastern basins of Afghanistan for the years with the lowest (2000 and 2008) and the highest (2016 and 2020) vegetation coverage from the studied period (2000-2021).



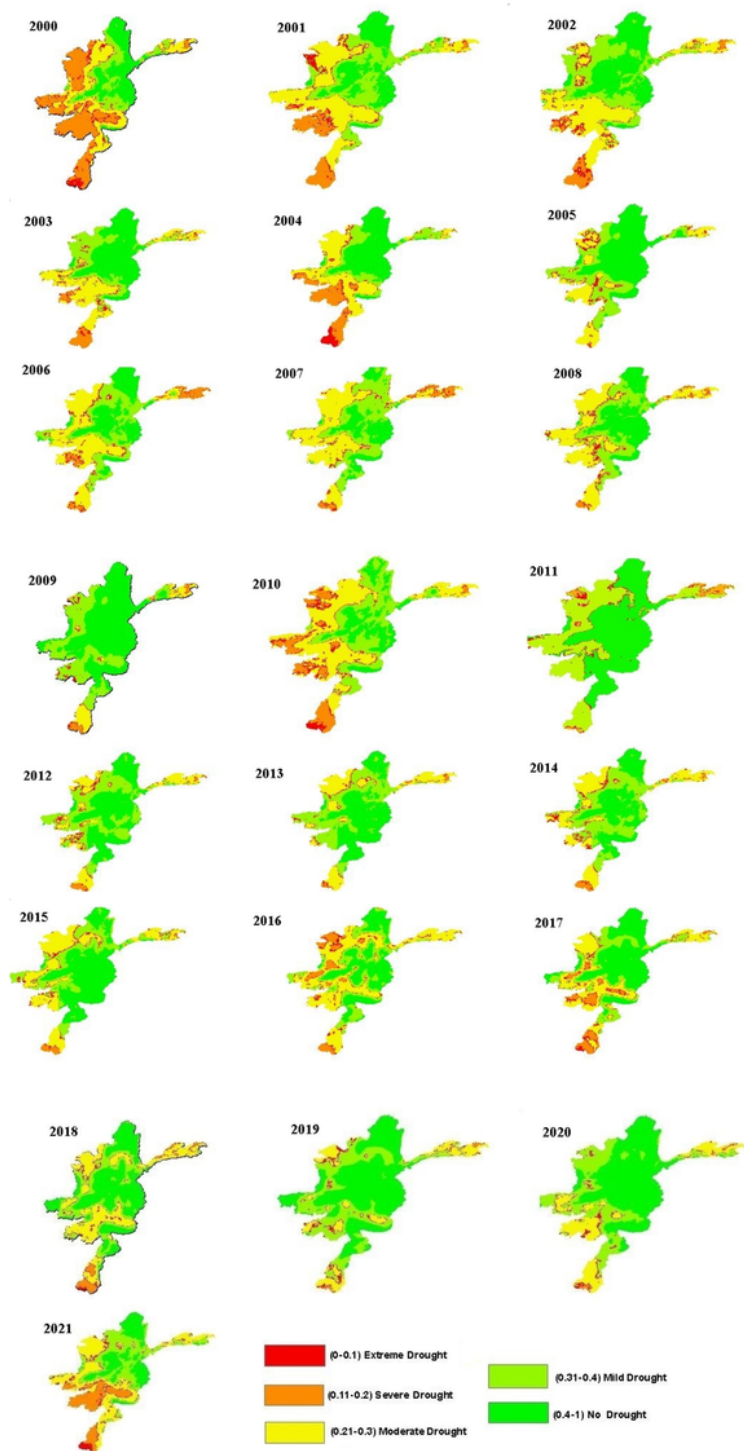


**Figure 7**

The maps of the spatial variations of meteorological drought expressed by the annual Microwave Integrated Drought Index in the eastern basins of Afghanistan for each year from the study period (2000-2021).

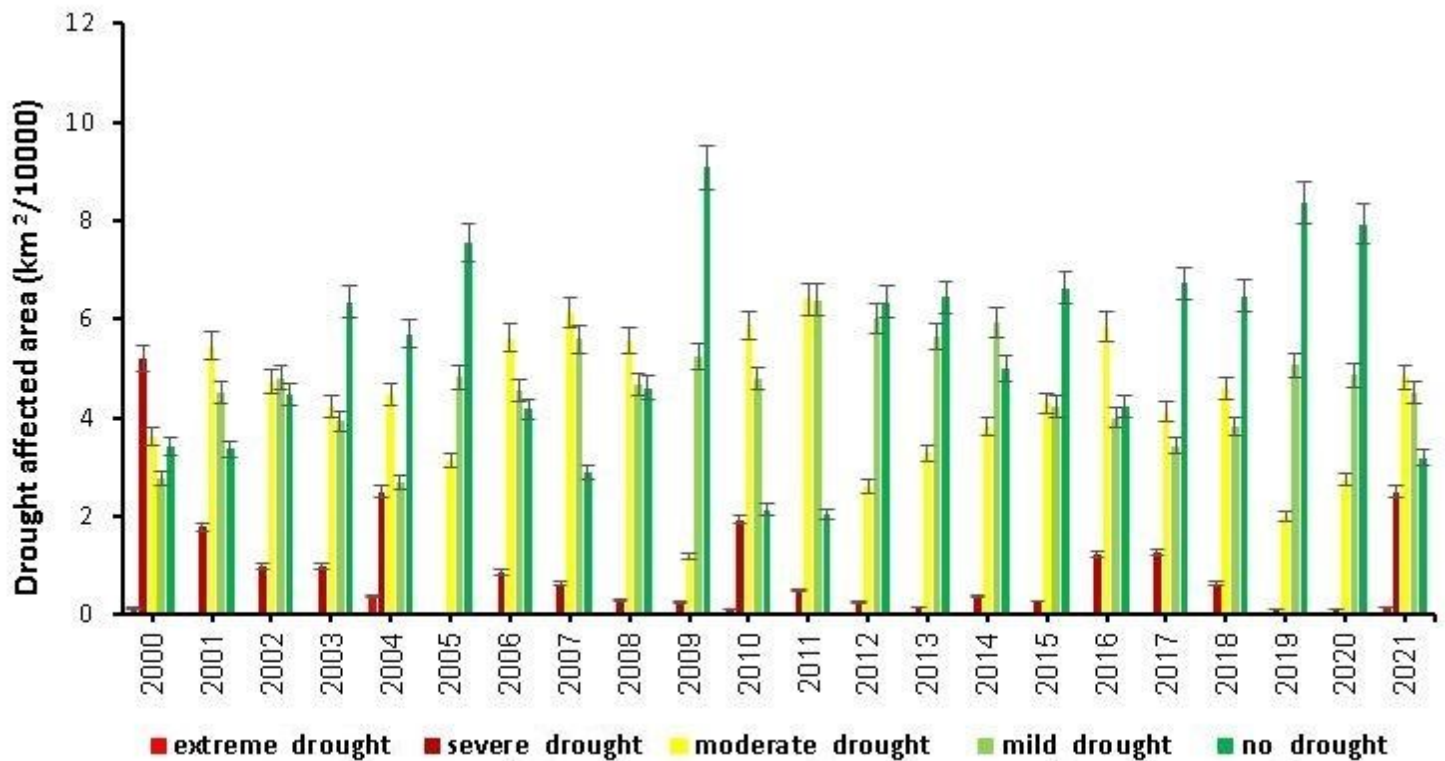


Figure 8

The temporal variations of meteorological drought expressed by the annual Microwave Integrated Drought Index in the eastern basins of Afghanistan during 2000-2021.

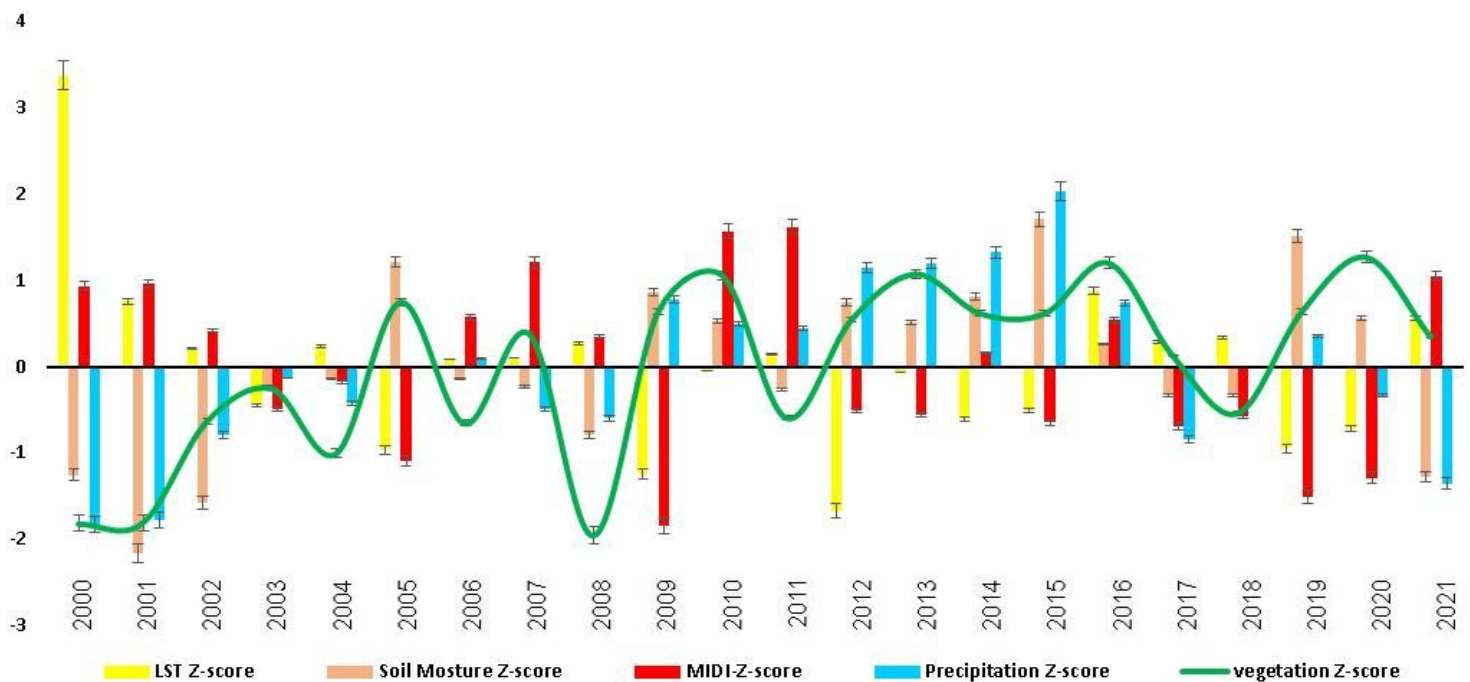
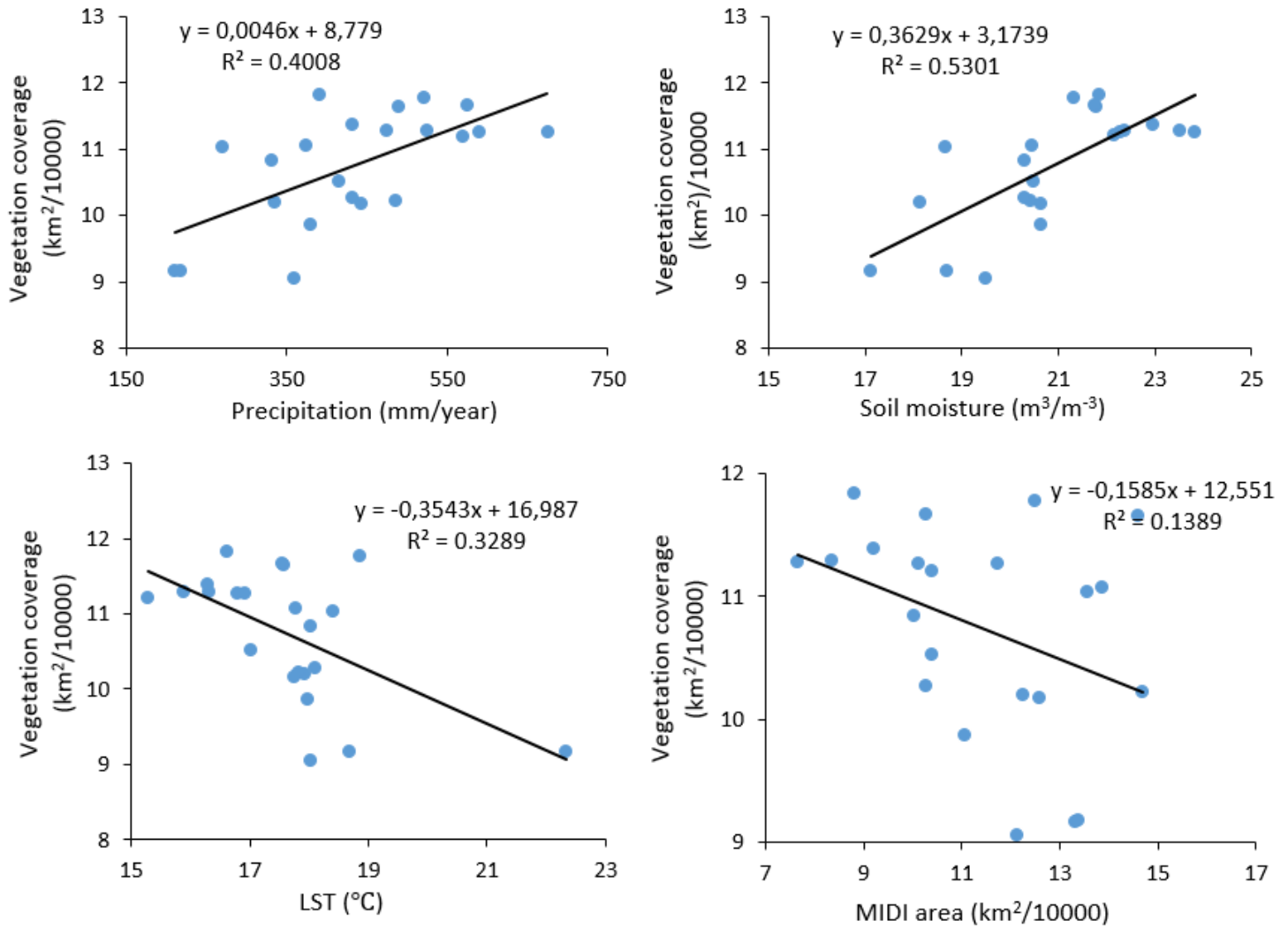


Figure 9

The annual anomalies of vegetation coverage, precipitation, soil moisture, LST, and MIDI for the eastern basins of Afghanistan during 2000-2021.



**Figure 10**

The scatter plots of the time series presenting the relationships between vegetation coverage and precipitation, soil moisture, LST, and MIDI for the eastern basins of Afghanistan during 2000-2021.

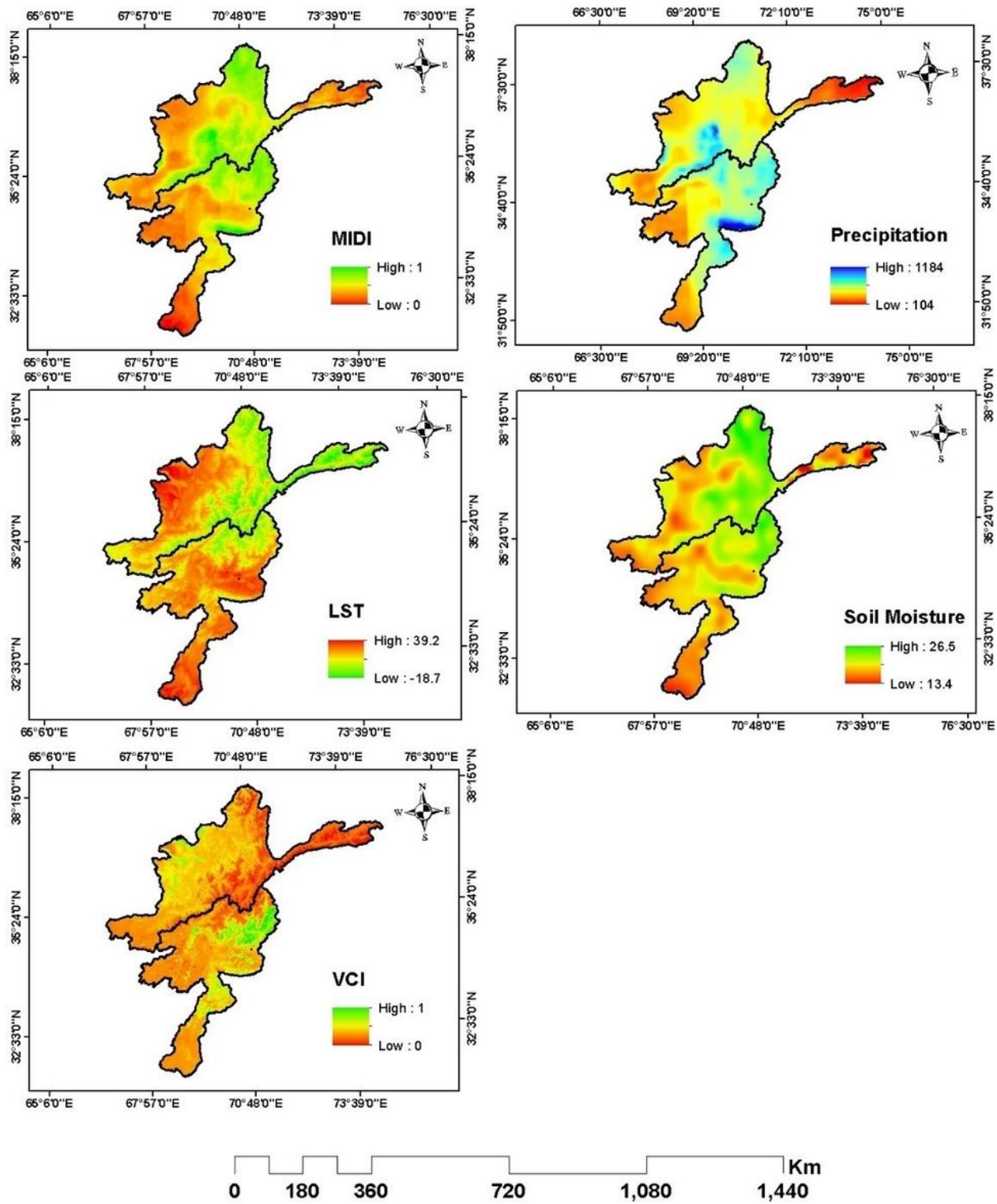


**Figure 11**

Spatial distributions of the mean precipitation, temperature, soil moisture, and drought index for the period from 2000 to 2021.

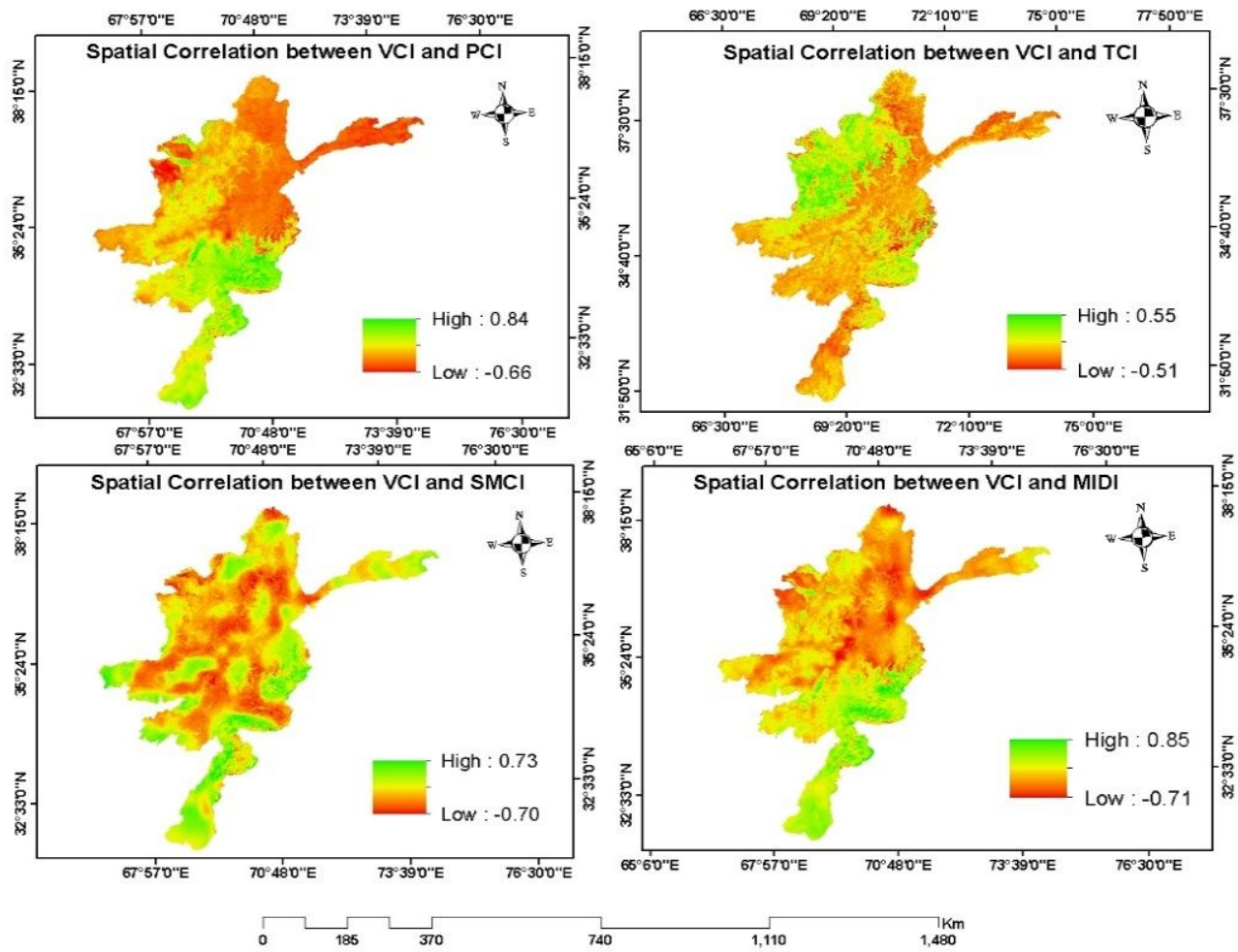


Figure 12

Spatial distribution of the correlation coefficients between the yearly mean of VCI and yearly means of the TCI, PCI, SMCI and MIDI.